ELSEVIER

Chemical Geology 192 (2002) 227–248

CHEMICAL GEOLOGY
INCLUDING
ISOTOPE GEOSCIENCE

www.elsevier.com/locate/chemgeo

Phase relations and the electrochemical determination of sulfur fugacity for selected reactions in the Cu–Fe–S and Fe–S systems at 1 bar and temperatures between 185 and 460 °C

John Lusk*, D. Maxwell Bray

Department of Physical Geography, Division of Environmental and Life Sciences, Macquarie University, Sydney N.S.W. 2109, Australia

Received 26 February 2002; accepted 9 July 2002

Abstract

Almost 30 years ago, Schneeberg [Econ. Geol. 68 (1973) 507] used the Ag/AgI/$Ag_{2+x}S$, $f_{S_{2(vapor)}}$ electrochemical cell for directly measuring the fugacity of sulfur vapor in equilibrium sulfide reaction mixtures in the Cu–Fe–S, Ni–S and Fe–S systems at temperatures between 210 and 445 °C. The present study has re-examined three of the reactions investigated by Schneeberg (1973), and expanded this work to include four others in the low-sulfur portion of the Cu–Fe–S system.

In sulfide ore assemblages the abundant iron sulfides pyrite (py) and/or pyrrhotite (po) are commonly associated with chalcopyrite (cp) and sphalerite. Other Cu–Fe–S sulfides, including covellite (cv), idaite (id), bornite (bn) and cubanite (cb), may also occur, but are less common because they require relatively high-sulfur or low-sulfur conditions in order to form. The range of $\log f_{S_2}$–temperature conditions that apply to most ore assemblages is therefore contained by reactions that involve these minerals. Accordingly, sulfur fugacities were determined for the following reactions: (1) py+Id=bn+S (sulfur vapor), (2) py+bn=cp+S, (3) py+cp=cb+S, (4) po+cp=cb+S, (5) py+cb=po+cb+S, (6) py+cp=po+cp+S and (7) py=po+S.

Our results for reaction (1) indicate lower sulfur fugacities than were obtained by Schneeberg (1973). For reactions (2) and (7), the present results show excellent agreement with those of Schneeberg (1973) at higher temperatures. However, at lower temperatures, previously undetected inflections in $\log f_{S_2}$ versus $1000/T$ plots occur at ~221 and ~237 °C for reactions (1) and (2), respectively. An invariant point occurs at ~335 °C and a sulfur fugacity of $\sim 10^{-9}$ where the phases py, cp, cb and po coexist with sulfur vapor. These results confirm earlier findings that reactions (3) and (5) occur above the invariant temperature and are replaced by reactions (4) and (6) below it. For the pyrite=pyrrhotite+S reaction (7), a previously unidentified inflection occurs at ~291 °C. The latter implies a phase transition in hexagonal pyrrhotite that appears to coincide with the lower temperature boundary of the sphalerite geobarometer. The present data provide a $\log f_{S_2}$–T framework that will facilitate future calibration of the FeS content in sphalerite.

Keywords: Sulfides; Sulfur fugacity; Experiments; Cu–Fe–S system; Phase relations

1. Introduction

Pyrite (py) and/or pyrrhotite (po) together with chalcopyrite (cp) and sphalerite are commonly asso-

* Corresponding author. Fax: +61-2-9850-8420.
E-mail address: luskjoru@bigpond.com.au (J. Lusk).

0009-2541/02/$ - see front matter © 2002 Published by Elsevier Science B.V.
PII: S0009-2541(02)00194-8

ciated in a variety of sulfide ore deposits. On the other hand, the copper–iron sulfides idaite (id), bornite (bn) and cubanite (cb) are notably less common because they reflect the more extreme conditions of ore formation, that is, relatively sulfur-rich or sulfur-poor conditions.

Sphalerite is extremely important in the present context because it can coexist with any of the above-mentioned minerals and is stable over a wide range of temperatures and pressures. Additionally, it is refractory and exhibits a large variation in FeS content ($\sim$0 to $\sim$35 mol%). The FeS content of sphalerite can be controlled by various reactions in the Cu–Fe–S system, and also by the pyrite = pyrrhotite + S (vapor) buffer reaction where it serves as an excellent geobarometer (Scott, 1973; Lusk and Ford, 1978; Hutchison and Scott, 1981). It is important to note, however, that only low concentrations of CuS occur in sphalerite, and that a similar situation applies to ZnS in relation to the iron and iron–copper (cubanite is an exception) sulfides where temperatures are below 500 °C. It should therefore be possible to use these reactions for calibrating the FeS content of sphalerite across the wide range of $\log f_{S_2}$–T conditions that determine phase relationships in the Cu–Fe–S and Fe–S systems.

The Cu–Fe–S system has received more attention than any other in sulfide geochemistry. A comprehensive study by Merwin and Lombard (1937) determined basic phase relations in the Cu–Fe–S system. Subsequent investigations within this complex system have been undertaken by many researchers, including Barton and Toulmin (1964a,b), Yund and Kullerud (1966), Mukaiyama and Izawa (1970), Cabri (1973), Barton (1973), Schneeberg (1973), Sugaki et al. (1975), Kojima and Sugaki (1985).

Merwin and Lombard (1937) achieved equilibrium with Cu–Fe–S mineral assemblages in the presence of vapor by independently controlling the sulfur vapor pressure. However, Barton and Toulmin (1964a,b) and Toulmin and Barton (1964) were the first to measure the sulfur fugacity of vapor in equilibrium with Cu–Fe–S and Fe–S assemblages, where the latter uniquely determine the sulfur fugacity. Their novel electrum tarnish method employed a range of Ag–Au alloys that were in direct communication with the sulfur vapor that was generated by a sulfide, or a sulfide mixture held at the same temperature. Unfortunately this method is extremely tedious, and becomes increasingly less sensitive with decreasing temperature and sulfur fugacity. Electrochemical methods were later applied by Sato (1971) and Schneeberg (1973). These contributions involved the Ag/AgI/$Ag_{2+x}S$, $fs_{2(g)}$ electrochemical cell that was developed and used much earlier by Rheinhold (1934) and Wagner (1953). Sato successfully measured sulfur fugacity directly in volcanic gases and Schneeberg measured sulfur fugacity over buffered sulfide reactions in evacuated Pyrex capsules. Schneeberg's (1973) method can yield excellent precision over the $\sim$200–460 °C range, and offers the advantage of continuous measurement. Cell voltages approach steady values in time–voltage plots where experiments are held at fixed temperatures. The attainment of equilibrium is assumed where voltage agreement is obtained, or closely approached, at chosen temperatures following cycling from both higher and lower temperatures.

Additionally, the method is especially valuable for studying reactions where mineral phases are unquenchable. Kissin and Scott (1979) employed Schneeberg's method for measuring the sulfur fugacity generated by a pyrrhotite crystal contained in a heated X-ray goniometer. Lusk (1989) adapted Schneeberg's method to determine equilibration temperatures for sulfide pairs. However, apart from these isolated studies, the electrochemical method for measuring sulfur fugacity has not been systematically applied to sulfide reactions since Schneeberg's (1973) pioneering contribution.

The present study has applied Schneeberg's (1973) method to seven geologically relevant Cu–Fe–S reactions with the primary aim of providing a refined and expanded map of $\log f_{S_2}$–temperature stability regions for the ternary sulfides idaite, bornite, chalcopyrite and cubanite that coexist with pyrite and/or pyrrhotite. Three of these reactions were investigated by Schneeberg (1973). They include the py + id = bn + S reaction that appears to be in error (cf. Barton, 1973), the py + bn = cp + S reaction that has been extensively investigated (e.g., Barton and Toulmin, 1964a,b; Czamanske, 1974; Kojima and Sugaki, 1985), and lastly the extremely important py = po + S reaction that has generated much discussion (cf. Czamanske, 1974; Scott and Barnes, 1971; Kissin and Scott, 1979; Barker and Parkes, 1986). The investigation of four

additional reactions in the iron-rich and sulfur-poor region of the Cu–Fe–S system completes the present study.

2. The electrochemical measurement of sulfur fugacity

The $Ag_{(s)}/AgI_{(s)}/Ag_{2+x(s)},fs_{2(g)}$ electrochemical cell is essentially a silver concentration cell that employs silver iodide as the solid electrolyte for the transference of silver ions (Ag^+). A pure silver electrode (negative polarity) fixes the chemical potential of silver at unity (i.e., μ_{Ag}=1) for all temperatures, and the composition of the very slightly non-stoichiometric argentite determines μ_{Ag} in the sulfide electrode. The latter is a function of cell temperature and the sulfur fugacity at this electrode. The transference number of silver ions in the AgI electrolyte is unity from 146 °C up to approximately 440 °C, beyond which electronic conduction becomes increasingly important (Schneeberg, 1973).

Wagner (1953) used the cell to measure sulfur fugacity across the stability field for argentite, where the silver content varies by not more than a few tenths of a percent. Argentite contains a slight excess of silver (i.e., $Ag_{2+x}S$) at the lowest measurable sulfur fugacities, but is essentially stoichiometric (i.e., Ag_2S) where it coexists with saturated sulfur vapor along the sulfur condensation curve. The excess silver occurs as interstitial defects (Rau, 1974). However, the small variation in silver content of the argentite equates to emf responses of 0 to ~220 and 0 to ~270 mV where temperatures are 178 and ~460 °C, respectively. This broad emf–temperature region is thus used routinely in the measurement of sulfur fugacity using Schneeberg (1973)- type cells.

The measured emf (ε) of a cell is closely related to the f_{S_2} in equilibrium with argentite (at ~1 bar) through the equation (Wagner, 1953; Sato, 1971):

$$\ln f_{S_2} = [\varepsilon - \varepsilon^0(T)]4F/RT + \ln f^0_{S_2}, \quad (1)$$

where $\varepsilon^0(T)$ is the emf (in volts) of the $Ag/AgI/Ag_2S, S_{(liquid)}$ reference cell at temperature T (Kelvin), $\ln f^0_{S_2}$ is the estimated fugacity of diatomic sulfur vapor ($S_{2(g)}$) in equilibrium liquid sulfur (S_l) at the same temperature, and R (1.9873 cal/deg. mol) and F (23.061 cal/V equiv.) are constants. However, choices are available among the published data sets for the reference state parameters $\varepsilon^0(T)$ and $\ln f^0_{S_{2(T)}}$, and those chosen uniquely determine the cell equation. For example, Schneeberg (1973) employed the $\ln f^0_{S_2}$ data of Rickert (1968) and his own unpublished data for ε^0 in obtaining the cell equation:

$$\log f_{S_2} = 1/T(20,158.6\varepsilon - 9099.7 \pm 103.2) + 3.73 \pm 0.034, \quad (2)$$

where the uncertainties are claimed to be standard deviations. A similar equation was derived by Sato (1971) who used data from Richardson and Jeffes (1952).

Cell life for this type of cell is shortened by long-term operation at high temperatures and/or by high sulfur fugacities. Nevertheless, brief excursions to ~490 °C have been successfully accomplished at the end of heating experiments. Examination of the silver electrodes at the end of experiments revealed an absence of sulfidation effects, but evidence of partial consumption after long periods of heating at the highest temperatures and at relatively high sulfur fugacities. This implies that additional silver sulfide, and/or silver sulfide iodide, formed in the electrolyte due to consumption of sulfur derived from the sulfide charge. The consumption of small quantities of sulfur is not likely to present a problem where buffered sulfidation reactions are involved, but could affect the composition of single sulfides. This in turn could lower sulfur fugacity in long-term experiments.

An intense darkening of the AgI electrolyte is commonly observed in cells after prolonged heating at higher temperatures. This suggests that black silver sulfide iodide, Ag_3SI (Reuter and Hardel, 1965), may have formed as a product in the AgI electrolyte that is usually a transparent yellow. This source of contamination was addressed by Schneeberg (1973), and further discussed by Kissin and Scott (1979). Schneeberg (1973) acknowledged small effects, but considered them to be within the precision of measurement. We concur with his assessment because reasonable agreement was obtained between repeated measurements made early and late in the lives of individual cells.

3. Experimental methods

3.1. Preparation of reaction mixtures

Eight sulfide reaction mixtures were prepared for use in the present sulfur fugacity experiments and in a companion study (manuscript in preparation). The latter involves a detailed determination of the compositions of sulfides in these buffer reactions, including those with and without sphalerite present.

The experimental mixtures comprised the following associations: (1) pyrite–idaite–bornite, (2) pyrite–bornite–chalcopyrite, (3) pyrite–chalcopyrite–cubanite, (4) pyrrhotite–chalcopyrite–cubanite, (5) pyrite–pyrrhoite–cubanite, (6) pyrite–pyrrhoite–chalcopyrite, (7) pyrite–pyrrhotite. These mixtures were finely ground immediately prior to use. Aliquots of the same mixtures were recrystallized in molten salt fluxes, and the products analyzed by microprobe in order to confirm the presence of phases reported for the respective mixtures.

The reaction mixtures were prepared by mixing appropriate proportions of sulfide minerals that were individually synthesized in evacuated Pyrex capsules. Pyrrhotite ($Fe_{(1-x)}$) and copper sulfides (CuS and Cu_2S) were produced by reacting sulfur powder (Aldrich Chemical prod. No. 21329—2; 99.998%) with hydrogen-reduced iron (Spex. Industries prod. No. FEO3; 99.999%) and copper (Spex. prod. No. CUO6; 99.999%) powders. These sulfides were reacted in appropriate proportions to yield the Cu–Fe–S sulfides idaite, bornite, chalcopyrite and cubanite. Pyrite was synthesized by reacting pyrrhotite with elemental sulfur to yield a product composed of ~99% pyrite.

Elemental reactants were first heated in a muffle furnace at around 250 °C for 8-week periods, followed by 3 weeks in a tube furnace at 400 °C. During the initial heating period all capsules were opened after 20–50 days and the sulfide products finely ground under acetone prior to resealing under vacuum. Pyrites were reground a second time at the end of the 8-week period and heated at 450 °C for an additional 2 weeks. Pyrrhotites of several compositions together with the synthetic chalcopyrites and cubanites received additional heating in Vycor capsules at temperatures to 600 °C.

A natural chalcopyrite–cubanite assemblage from the Cobar C.S.A. Mine (N.S.W.) was substituted in the mixture containing synthetic chalcopyrite and cubanite. This action was taken following an initial set of experiments in which cell behavior was found to be extremely erratic, apparently due to an unresolved synthesis problem involving cubanite (cf. Cabri, 1973). The substituted assemblage contained approximately equal proportions of natural chalcopyrite and cubanite, together with traces of pyrrhotite and bismuth.

3.2. Electrochemical cells

3.2.1. Cell designs

Two variants of electrochemical cell design were used in the present study. Fig. 1a shows the cell design that was used for obtaining E^0 data in the sulfur condensation experiments. It contains a relatively large sulfur reservoir that is positioned as close as possible to the electrodes, thus minimizing the effects of longitudinal thermal gradients. Fig. 1b shows the cell design that was employed for routine sulfur fugacity measurements. This cell is essentially the same as described by Schneeberg (1973), although a number of changes in technique were adopted in fabricating the former.

Pyrex tubing, 6×2.2 mm (bore), was used for containment of the silver iodide electrolyte in all cells. Tubing of this size was found to be relatively effective in resisting cracking when silver iodide cooled below its ~153 °C transition temperature. Cells for routine measurement of sulfur fugacity were prepared from ~130 mm lengths of this tubing. One end was flared and glass blown onto an ~80 mm length of 10×7.5 mm (bore) tubing for final attachment to a vacuum line. The cells for ε^0 measurements were glass blown from several sizes of tubing, namely, ~40 mm lengths of 6×2.2 mm tubing (to accommodate both electrodes separated by the electrolyte), ~30 mm lengths of 10×7 mm tubing (to accommodate ~300 mg of sulfur), ~60 mm lengths of 6×2.2 mm tubing (to carry the glass-coated positive electrode conductor and to aid in sealing), and finally ~80 mm lengths of 10×7 mm tubing for connection to a vacuum line.

3.2.2. Fabrication of electrodes

The electrodes were made from ~90 mm lengths of 0.2 mm diameter platinum wire (thermocouple grade) that terminated in silver or silver sulfide

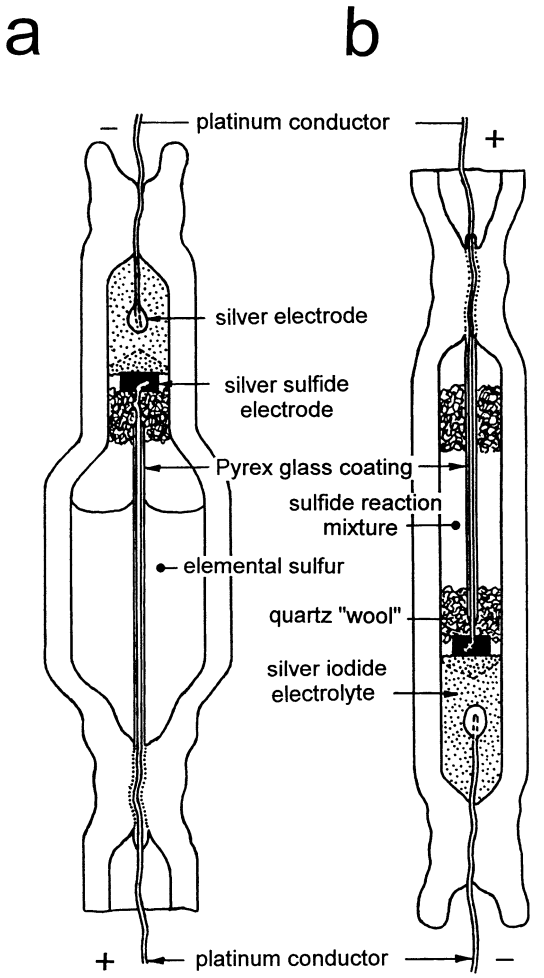

Fig. 1. Cell designs used in the electrochemical measurements. (a) Cell used for E^0 calibration; (b) cell employed for routine measurement of sulfur fugacity.

electrodes. The conductor wire for the silver sulfide electrode was sheathed with Pyrex glass, except for 5 and 25 mm lengths at the free ends. The coating was accomplished by first drawing out glass capillaries, breaking to 60 mm lengths, threading onto the conductors, and then slowly drawing the stretched (and inclined) wires through a flame to soften and collapse the glass onto the wires. The glass sheathing prevents the positive electrode conductors from directly contacting the powdered sulfide mixtures (Schneeberg, 1973), or the liquid sulfur through which they pass. Coating of the negative conductor wires was not required.

The silver electrodes were fabricated in two ways. For routine sulfur fugacity measurements involving the sulfide reactions, pieces of silver (Spex. Industries prod. No. AGO8; 99.9999%) weighing approximately 10 mg were cut from silver shot and melted with a flame to produce molten balls supported in depressions on a flat graphite substrate. The heated ends of platinum conductors were quickly immersed into molten silver balls and withdrawn from the flame with the balls attached, as was described by Schneeberg (1973). However, some degree of alloying between silver and platinum is likely using this method, and could yield alloys containing ≤20 wt.% platinum in worst cases. This in turn will reduce the activity of Ag in the "silver" electrode, and thus affect emf measurements. A test set of silver–platinum electrodes of known alloy compositions (i.e., 10, 18, 25, 30 and 33 wt.% Pt) was prepared in order to investigate the effect of alloying on a qualitative basis. This was achieved by slicing pure silver balls almost through, and crimping them tightly around the proximal ends of the platinum conductors. The same method was used in preparing the test set of alloy electrodes.

The silver sulfide electrodes were prepared by compressing ~30 mg aliquots of silver sulfide filings into 1.8 mm diameter pellets with ~8 mm lengths of platinum wire (sharply bent or welded into a ball at the buried end) extending from their top centers. The wire extensions from the pellets were arc welded onto the glass-free ends of the 90 mm lengths of platinum conductor wires.

3.2.3. Method of cell assembly

A silver electrode was inserted ~25 mm inside the open end of 6×2 mm Pyrex tubing that was mounted vertically, and the electrode wire bent over for support. The tubing was heated circumferentially to soften the glass, and tweezers used to assist in collapsing the glass onto the platinum wire ~10 mm back from the ball electrode. The glass seal surrounding the silver electrode conductor was then thoroughly annealed with a gas torch. A stainless steel rod cut obliquely across its end was used to center the electrode within the bore of the tubing.

Light sensitive silver iodide powder (Cerac Chemical; 99.99%) was added incrementally to cover the

Table 1
Voltage measurements for the sulfur condensation reaction

Measurement identification[a]	Temperature (K)	Millivolts (mV)	Error (mV, 1σ)
1—(13.6)/4	460	223.90	0.16
2—(15.2)/4	475	226.29	0.17
3—(16.2)/4	490	228.54	0.17
4—(17.4)/4	502	230.39	0.09
5—(18.7)/4	515	232.45	0.06
6—(19.5)/4	528	234.58	0.05
7—(20.8)/4	543	236.90	0.07
8—(22.2)/4	559	239.30	0.09
9—(23.1)/4	578	242.27	0.07
10—(24.2)/3	608	247.42	0.13
11—(25.3)/2	637	252.42	0.04
12—(26.1)/2	664	256.54	0.07
13—(27.0)/2	702	262.34	0.07

[a] For 3—(16.2)/4: 3=position in measurement sequence; (16.2)=time elapsed in hours; /4=number of cells used.

silver electrode, and followed each time by melting under low lighting conditions. Rapid flicks of the hand-held cells facilitated the downward movement of the molten silver iodide. When the silver electrode was buried in the solid silver iodide to a depth of ~3 mm, a layer (~1 mm thick) of powdered AgI was added and tamped down to produce a flat surface on which the silver sulfide electrode is supported (Schneeberg, 1973). The silver sulfide electrode was then carefully inserted into the cell, and anchored in place with a small wad of quartz wool. Around 125 mg of finely ground sulfide mixture was added and held in place by a second wad of quartz wool. After evacuating down to around $5-7\times10^{-5}$ atm over a period of about 10–15 min, approximately 15 mm lengths of the 6 mm glass tubing toward the top ends of cells were collapsed and sealed off with a gas flame.

The completed cells were wrapped in aluminum foil and stored in a dark environment prior to use. Shorting of the cells was not possible because the positive leads were insulated from external contact by the glass extensions at the top ends of the cells. The latter were cut off to yield overall cell lengths of 110–115 mm immediately prior to loading in furnaces. Approximately one in eight of the stored cells was unusable due to stress cracking of the Pyrex glass in the vicinity of the contained electrolyte.

3.3. Loading cells

Six cells at a time were loaded into drilled aluminum sample holders (45 mm (diam.)×130 mm

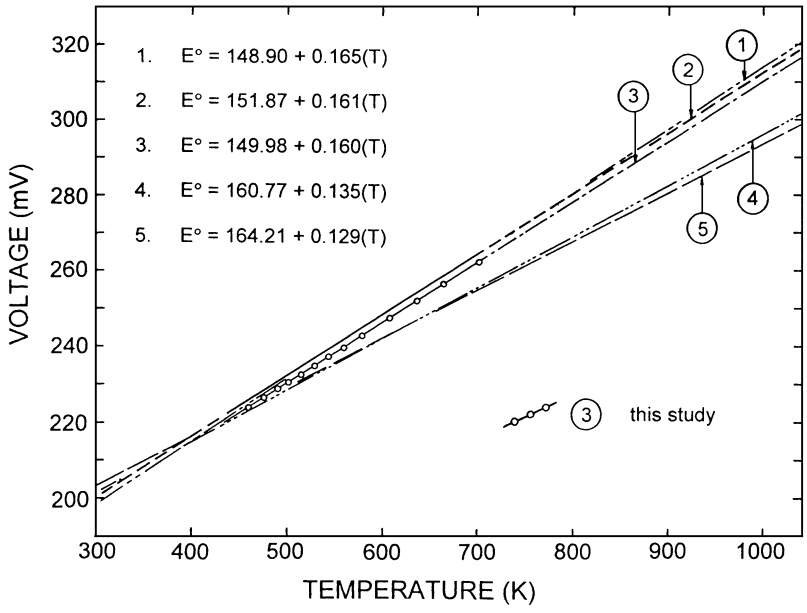

Fig. 2. Electrochemical determinations of E^0 (mV) for the sulfur condensation reaction. Attributions for Eqs. (1), (2) and (4), (5) are given in the text.

(length)) provided with end caps held in place with screws. The platinum conductor wires from the silver electrodes were twisted together with an insulated platinum wire (i.e., the common negative) that passed upward through a hole in the center of the cylinder. The positive leads from the silver sulfide electrodes were insulated from each other using twin bore alumina tubing. The positive leads were arc welded to extension conductors that also passed upward through the top end cap of the aluminum containment cylinder.

After loading, the sample holders were wrapped in 2 mm thick Kaowool paper and suspended by wires from the tops of the vertical tube furnaces. However, for the sulfur condensation experiments, it was necessary to invert the cells so that liquid sulfur could not make direct contact with the positive electrode or with the electrolyte. The bottom end spaces of the 330 mm long (50 mm bore) tube furnaces were plugged loosely with Kaowool to minimize convection. Custom-built temperature controllers in conjunction with voltage regulators on the output side were used to heat the furnaces. Pt/Pt13Rh thermocouples were used with a Kaye ice point reference station for control and measurement functions.

3.4. Temperature and voltage measurements

Temperatures were measured with annealed Pt/Pt13Rh thermocouples that were sealed in evacuated Pyrex tubing of the same size as was used in the cells. These were calibrated initially against the melting points of tin, cadmium and zinc metals, and checked against a platinum resistance thermometer at the end of the experiments. Thermocouple voltages were measured with a Keithley 196 digital multimeter. Temperature measurements are accurate to better than ± 0.5 °C over the temperature range of interest.

The cell reaction mixtures were held at the highest temperature locations in the sample blocks. Temperature gradients over the respective 20–25 mm lengths were found to be less than 1° at 450 °C. An overall accuracy of approximately ± 1 °C is estimated for the experimental data where measurement and thermal gradient errors are taken into account.

Cell voltages were measured in forward and reverse directions using a varacator bridge electrometer (Analog Devices model 311K) in conjunction with a digital voltmeter (Analog Devices model AD2024). This combination of instruments effectively prevents degrading, or the occurrence of detectable chemical changes within cells. The electrometer delivers an extremely low current during the short periods of measurement, and all of the voltmeters used indicate true voltages because their input impedances (>40 MΩ) are many orders of magnitude larger than cell resistance values. The measured voltages were checked against those obtained with two precision instruments, including a Keithley model 181 nanovoltmeter and a Hewlett-Packard model 3468A multi-

Table 2
Sulfur fugacity measurements for the pyrite+idaite=bornite+sulfur (vapor) reaction

Measurement details[a]	Temperature (°C)	Temperature 1000/K	Cell voltage (ε, mV$\pm 1\sigma$)	Sulfur fugacity[b] $\log f_{S_2}$ ($\pm 1\sigma$)
A. Data above the inflection point				
5—(1/8)/4	448	1.387	252.4±0.4	−1.99±0.01
4—(2/7)/4	423	1.436	241.8±0.3	−2.50±0.01
33—(1/127)/4	410	1.464	237.0±0.3	−2.76±0.01
3—(2/5)/4	400	1.486	232.4±0.1	−3.00±0.01
7—(6/14)/4	391	1.505	228.3±0.4	−3.21±0.01
2—(2/3)/4	379	1.533	224.6±0.3	−3.45±0.01
8—(2/16)/4	371	1.553	219.8±0.4	−3.69±0.01
1—(1/1)/4	362	1.575	217.0±0.2	−3.89±0.01
10—(4/21)/4	335	1.644	205.0±0.4	−4.62±0.01
31—(2/124)/4	322	1.681	200.9±0.4	−4.95±0.01
11—(2/24)/4	318	1.693	197.6±0.5	−5.12±0.01
12—(4/28)/4	301	1.740	191.3±0.7	−5.59±0.02
30—(3/122)/4	291	1.772	187.6±0.6	−5.90±0.02
13—(2/30)/4	285	1.790	184.4±0.5	−6.11±0.02
14—(2/32)/4	272	1.833	178.9±0.7	−6.55±0.03
15—(3/35)/4	270	1.841	177.6±0.9	−6.65±0.03
16—(1/36)/4	258	1.882	172.8±1.2	−7.06±0.05
17—(3/39)/4	245	1.929	167.5±1.9	−7.53±0.09
29—(6/119)/4	240	1.947	164.3±2.9	−7.77±0.11
18—(4/43)/4	237	1.961	164.2±2.4	−7.85±0.09
19—(8/51)4	231	1.982	161.0±3.6	−8.10±0.14
28—(15/113)/4	228	1.995	158.8±4.1	−8.27±0.16
B. Data below the inflection point				
22—(4/69)/4	209	2.076	159.0±2.5	−8.75±0.10
23—(5/73)/4	203	2.101	159.8±2.5	−8.87±0.11
24—(4/77)/4	195	2.136	160.8±2.8	−9.03±0.12
25—(8/85)/4	187	2.174	162.2±4.5	−9.20±0.20

[a] In 28—(15/113)/4, for example, 28—=position in measuring sequence; (15=days at respective temperature before measurement accepted; /113=total days from commencement of heating experiments.

[b] Sulfur fugacities calculated from the present cell equation: $\log f_{S_2} = [20,158.6\varepsilon - 97229]1/T + 3.76$, where ε is in volts.

meter. These instruments (±0.05 mV accuracy; >1 GΩ impedance) gave readings that agreed to within 0.01 mV. The AD2024 voltmeter, with a reading precision of 0.1 mV, gave voltage readings that were 0.1–0.25 mV lower over the same range. Because these differences are well within the limits of error for the sulfide reaction experiments, the relevant voltage data have not been corrected. A precision instrument was used in measuring voltages for the sulfur condensation experiments.

Voltage data were obtained by cycling up and down in temperature using incremental steps over long periods of time. Experiments were held at chosen temperatures until steady voltages were attained, or closely approached, as suggested in daily time–voltage plots. It was found to be advantageous to increase or decrease the temperature by ~5 °C increments for most reactions at lower temperatures, and also for reactions with inherently low sulfur fugacities. Temperature changes of 20 °C or more are to be avoided because they typically result in erratic voltage responses that require long periods for recovery. For sluggish reactions, it is also useful to dedicate one set of cells to the higher temperature part of a given reaction, and a matching set to the lower temperature part.

Individual cells respond erratically where they are accidentally shorted-out. Others in normal usage can deviate from normal behavior for some time, and then self-correct. Where abnormal behavior was detected, the measurements in question were rejected. Mean voltages and standard deviations are reported where full sets or part sets of cells behaved normally, that is, gave similar voltages that differed usually by not more than a few millivolts. This selection process accounts for the variation in cell numbers that are indicated in the tables following.

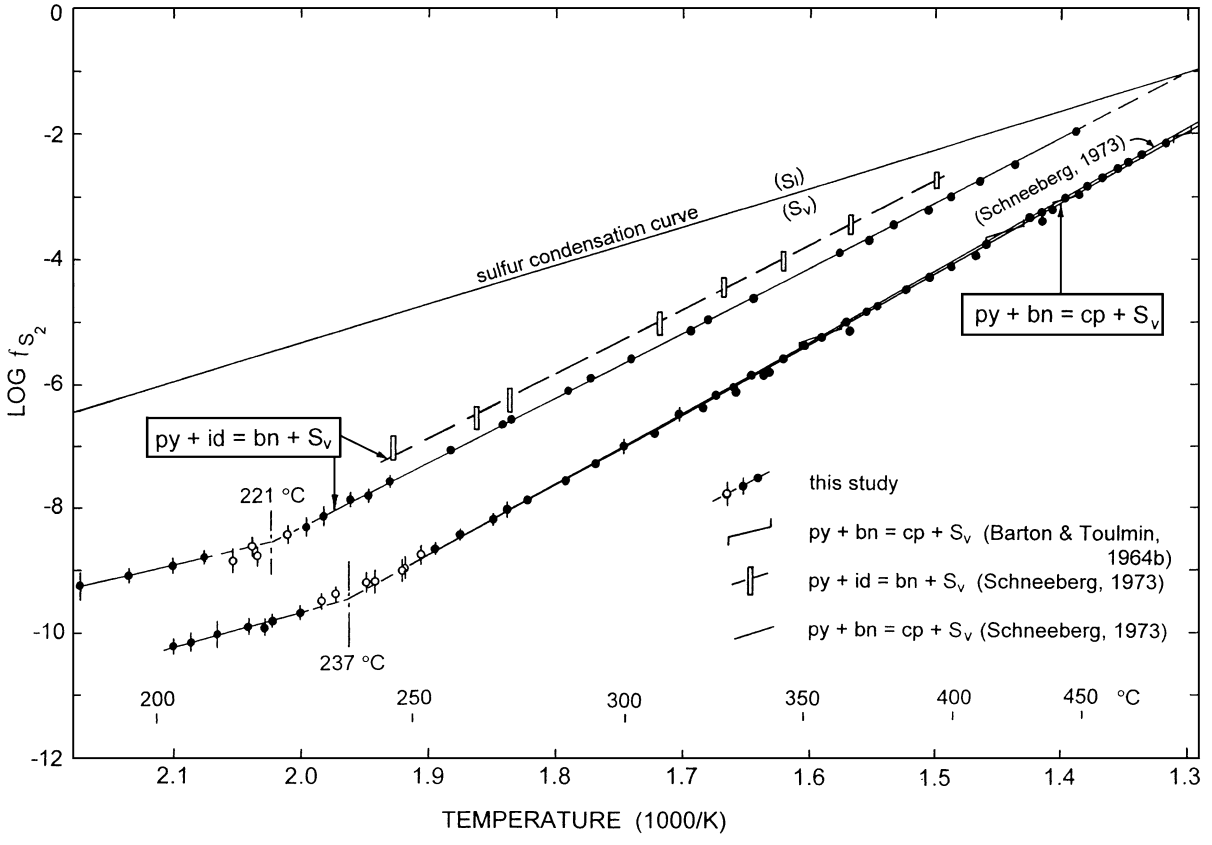

Fig. 3. Sulfur fugacity versus 1000/T plots for the pyrite + idaite = bornite + sulfur (vapor) and pyrite + bornite = chalcopyrite + sulfur (vapor) reactions. Data represented by the empty symbols have been excluded from the regression analyses.

4. Results

4.1. The sulfur condensation reaction

Sequential measurements were made for the sulfur condensation reaction at temperatures between 187 and 429 °C. The results presented in Table 1 were obtained from a set of six cells with mechanically crimped pure silver electrodes. Data was accepted for four of the cells at the lower temperatures, but from only two cells at the highest temperatures. These cells gave stable voltages with small differences at the various temperatures.

A notable feature of these experiments was the rapidity with which steady voltages were attained after making temperature changes. This allowed sets of stable measurements to be obtained within 40 to 80 minute intervals. Forward and reverse voltages differed usually by not more than 1 or 2 tenths of a millivolt for individual cells. Differences between cells were typically less than 1 mV, and commonly not more than a few tenths.

Inspection of the cells at the end of the experiments revealed that the ~300 mg samples of sulfur had a slightly brownish color, suggesting contamination by elemental iodine. This evidently occurred through

Table 3
Least squares best-fit equations

Reaction	Temp. range (°C)	Least squares fit	Standard error of estimate	R^2	Source
1a. Sulfur condensation	187–428	$E^0=149.98+0.1603\times(T)$	0.20	0.9997	this study (Eq. (3), Fig. 2)
1b. Sulfur condensation[a]	150–425	$E^0=151.87+0.1607\times(T)$	0.15	0.9999	Kiukkola and Wagner (1957) (Eq. (2), Fig. 2)
2a. py+id=bn_{cub}+S	228–448	$\log f_{S_2}=12.296-1.0286\times10^4(1/T)$	0.02	0.9999	this study
2b. py+id=bn_{tet}+S	187–209	$\log f_{S_2}=0.826-0.4613\times10^4(1/T)$	0.00	0.9994	this study
2c. py+id=bn_{cub}+S[b]	327–394	$\log f_{S_2}=12.491-1.0185\times10^4(1/T)$	0.05	0.9986	Schneeberg (1973)
3a. py+bn_{cub}=cp+S	255–486	$\log f_{S_2}=12.637-1.1243\times10^4(1/T)$	0.05	0.9993	this study
3b. py+bn_{tet}=cp+S	206–225	$\log f_{S_2}=1.2418-0.5439\times10^4(1/T)$	0.02	0.9782	this study
3c. py+bn_{cub}=cp+S[b]	279–445	$\log f_{S_2}=12.811-1.1328\times10^4(1/T)$	0.05	0.9946	Schneeberg (1973)
4a. py+cp=cb+S	334–488	$\log f_{S_2}=16.849-1.5563\times10^4(1/T)$	0.03	0.9996	this study
4b. py+cp=po+cp+S	268–328	$\log f_{S_2}=10.97-1.1994\times10^4(1/T)$	0.04	0.9959	this study
4c. py+cb=po+cb+S	334–488	$\log f_{S_2}=15.52-1.522\times10^4(1/T)$	0.02	0.9998	this study
4d. cp+po=cb+S	268–312	$\log f_{S_2}=10.796-1.2299\times10^4(1/T)$	0.08	0.9779	this study
5a. py=po+S	330–448	$\log f_{S_2}=14.594-1.4654\times10^4(1/T)$	0.04	0.9987	this study
5b. py=po+S	294–448	$\log f_{S_2}=14.557-1.4628\times10^4(1/T)$	0.04	0.9994	this study
5c. py=po+S[c]	294–324	$\log f_{S_2}=14.618-1.4663\times10^4(1/T)$	0.04	0.9930	combined data
5d. py=po+S	243–286	$\log f_{S_2}=12.45-1.3431\times10^4(1/T)$	0.01	0.9995	this study
5e. py=po+S[a,c]	294–742	$\log f_{S_2}=19.007-2.2119\times10^4(1/T)+1.8602\times10^6(1/T)^2$	0.06	0.9997	combined data
6a. po (N_{FeS}=0.9464)	330–422	$\log f_{S_2}=9.1127-1.1404\times10^4(1/T)$	0.06	0.9954	this study
6b. po (N_{FeS}=0.9480)	355–434	$\log f_{S_2}=8.7226-1.1255\times10^4(1/T)$	0.07	0.9847	this study
6c. po (N_{FeS}=0.9545)	299–440	$\log f_{S_2}=8.8819-1.1804\times10^4(1/T)$	0.04	0.9991	this study
6d. po (N_{FeS}=0.9625)	388–456	$\log f_{S_2}=7.9256-1.183\times10^4(1/T)$	0.02	0.9990	this study

All $\log f_{S_2}$ data have been calculated using the present cell equation.

[a] Equation is based on smoothed data, or includes smoothed data.

[b] Data below an unidentified inflection point has been excluded from the analysis.

[c] Includes data from two or more sources.

iodine vapor transfer from the AgI electrolyte because the inverted cell orientation prevented the liquid sulfur from directly contacting the silver sulfide electrodes or the solid electrolyte.

A companion set of experiments involved cells with crimped Ag–Pt alloy (i.e., 10, 18, 25, 30 and 33 wt.% Pt) electrodes. Cells with the higher Pt contents generated lower voltages (≤15 mV), behaved erratically, and were not reproducible. However, a pair of cells containing ~10 wt.% Pt proved to be an exception. They gave steady and reproducible voltages that were ~0 to 1 mV lower than for cells with the pure silver electrodes. These qualitative tests suggest that an alloying of ≤10 wt.% Pt in silver electrodes has little effect on cell voltages (i.e., ≤1 mV), or on cell stability. However, lower voltages and instability can be anticipated where the degree of alloying is higher. This potential source of uncertainty can be avoided by using pure silver electrodes in conjunction with the crimping method of construction.

4.2. Choice of parameters for a cell equation

E^0 (or ε^0) values relate cell voltage to total sulfur pressure for the sulfur condensation reaction over a temperature range of interest. Fig. 2 shows the present ε^0 data together with linear plots for four alternative data sets. The linear plots occur in two distinct groups. The plots for (1) Schneeberg (1973), (2) Kiukkola and Wagner (1957), and (3) the present study are tightly grouped and have steeper slopes. The second group contains the data of (4) Browner (1987) and (5) Rickert (1982). The effective ε^0 equation used by Schneeberg was derived from his cell equation by subtracting the $\log f^0_{S_2}$ data of Rickert (1968).

The two groups of data cross around 400 K and have voltages that are separated by ~20 mV at 1000 K. It is therefore evident that one of these groups is seriously in error. The accuracy of individual equations can be assessed by first determining the free energy of formation for argentite using additional data for sulfur that was sourced from Rau et al. (1973a,b). The free energy values obtained are then compared with the high-quality free energy data for argentite reported by Kubaschewski et al. (1967). Eqs. (1)–(3) yield Δf values between 473 and 1020 K that are within 0.45 kcal (or ≤1.8%) of the values determined from data given in Kubaschewski et al. (1967).

Table 4
Sulfur fugacity measurements for the bornite+pyrite=chalcopyrite+sulfur (vapor) reaction

Measurement details	Temperature		Cell voltage (ε, mV±1σ)	Sulfur fugacity $\log f_{S_2}$ (±1σ)
	(°C)	1000/K		
A. Data above the inflection point				
36—(2/290)/2	486	1.317	236.0±0.7	−2.14±0.01
35—(3/288)/2	475	1.336	231.5±0.8	−2.34±0.01
29—(4/248)/3	470	1.346	228.5±0.3	−2.46±0.01
28—(5/244)/2	465	1.355	226.3±0.2	−2.57±0.01
27—(7/239)/2	458	1.367	223.3±0.3	−2.71±0.01
30—(7/255)/2	452	1.379	220.6±0.7	−2.84±0.01
26—(3/232)/3	449	1.385	216.5±3.1	−2.98±0.04
31—(6/261)/2	443	1.396	217.2±0.4	−3.01±0.01
25—(4/229)/3	438	1.406	211.8±3.2	−3.22±0.05
24—(6/225)/4	433	1.415	207.0±5.1	−3.40±0.05
32—(6/267)/2	433	1.416	212.7±0.3	−3.24±0.01
33—(7/274)/2	429	1.425	211.0±0.4	−3.33±0.01
34—(11/285)/2	412	1.459	202.7±1.3	−3.75±0.02
20—(10/201)/6	409	1.467	197.7±2.5	−3.93±0.05
19—(7/191)/6	399	1.487	195.4±1.7	−4.11±0.04
18—(8/184)/6	392	1.504	192.3±1.8	−4.29±0.04
17—(7/176)/6	384	1.523	189.6±1.3	−4.48±0.05
16—(7/169)/6	374	1.546	185.1±1.8	−4.74±0.05
15—(7/162)/6	370	1.555	184.2±1.1	−4.82±0.03
3—(14/44)/6	364	1.568	177.1±3.4	−5.12±0.10
14—(7/155)/5	363	1.571	181.9±1.2	−4.99±0.05
13—(7/148)/6	355	1.591	177.9±2.3	−5.22±0.06
12—(7/141)/6	350	1.604	176.0±1.9	−5.35±0.05
11—(5/134)/6	344	1.621	173.1±1.8	−5.55±0.06
2—(9/30)/8	340	1.632	167.6±3.9	−5.79±0.10
32—(7/351)/7	338	1.636	166.6±2.6	−5.85±0.09
10—(6/129)/7	334	1.646	168.7±2.8	−5.84±0.09
31—(4/344)/7	330	1.658	163.0±2.0	−6.10±0.07
1—(21/21)/6	330	1.659	165.8±2.8	−6.01±0.10
9—(7/123)/6	329	1.660	165.8±2.5	−6.02±0.09
8—(7/116)/7	324	1.674	164.2±2.5	−6.15±0.09
30—(4/340)/7	321	1.684	159.8±1.4	−6.36± 0.06
7—(4/109)/7	314	1.703	159.9±2.8	−6.47±0.10
29—(4/336)/6	308	1.722	154.8±1.2	−6.76±0.05
6—(6/105)/6	299	1.746	153.3±3.2	−6.96±0.10
28—(10/332)/6	292	1.768	148.8±1.6	−7.26±0.07
27—(4/322)/5	285	1.792	145.4±1.7	−7.53±0.08
26—(4/318)/5	276	1.822	142.0±2.0	−7.84±0.08
5—(53/99)/6	271	1.838	140.7±3.4	−7.99±0.10
25—(16/314)/5	268	1.849	138.7±2.1	−8.14±0.08
14—(11/20)/7	260	1.875	136.3±2.7	−8.39±0.11
24—(8/298)/5	255	1.894	133.7±2.8	−8.62±0.11
B. Data below the inflection point				
18—(4/232)/6	225	2.006	126.3±2.5	−9.65±0.10
19—(10/242)/6	221	2.022	125.5±2.5	−9.79±0.10
20—(11/253)/7	217	2.040	126.8±3.8	−9.86±0.15
8—(14/135)/4	217	2.042	126.9±0.9	−9.87±0.05
9—(8/143)/4	211	2.065	127.8±1.3	−9.98±0.05
21—(12/265)/5	211	2.066	128.4±5.9	−9.97±0.25
22—(8/273)/5	206	2.086	127.7±3.1	−10.12±0.15

Among these, Eqs. (2) and (3) yield the most consistent differences, but the data of Kiukkola and Wagner (1957) show the smallest departures (i.e., 0.5% at 1020 K and 1.0% at 473 K). Furthermore, Thompson and Flengas (1971) obtained good agreement between their own free energy of formation data for argentite and determinations obtained using extrapolations of Kiukkola and Wagner's (1957) data to temperatures between 500 and 800 °C.

Choosing the most accurate $\log f^{0}_{S_{2(T)}}$ data for inclusion in a working cell equation is a vexed problem. The first requirement is to select the most accurate total sulfur pressure data for the sulfur condensation reaction over the temperature range of interest. The second requirement is to choose between data sets that attempt to estimate the partial pressures for 7 or more important molecular sulfur species in sulfur vapor. The relative abundances of these species change in a complex manner with both temperature and total pressure. In spite of these difficulties, the S_2 molecular species predominates where total sulfur pressures are less than $\sim 10^{-2}$ bar.

Barton and Skinner (1979) suggested that the total sulfur vapor pressure data of West and Menzies (1929) is the most accurate from 200 to 500 °C, and that of Rau et al. (1973a) for higher temperatures. Barton and Skinner (1979) have obtained an excellent fit to these separate data sets where each is combined with Rau et al.'s (1973b) polymerization model for sulfur vapor.

In the present study, we have chosen to use the cell equation

$$\log f_{S_2} = [20,158.6\varepsilon - 9,229.0]1/T + 3.76 \qquad (3)$$

that is based on the ε^0 data of Kiukkola and Wagner (1957) and the sulfur polymerization model of Rau et

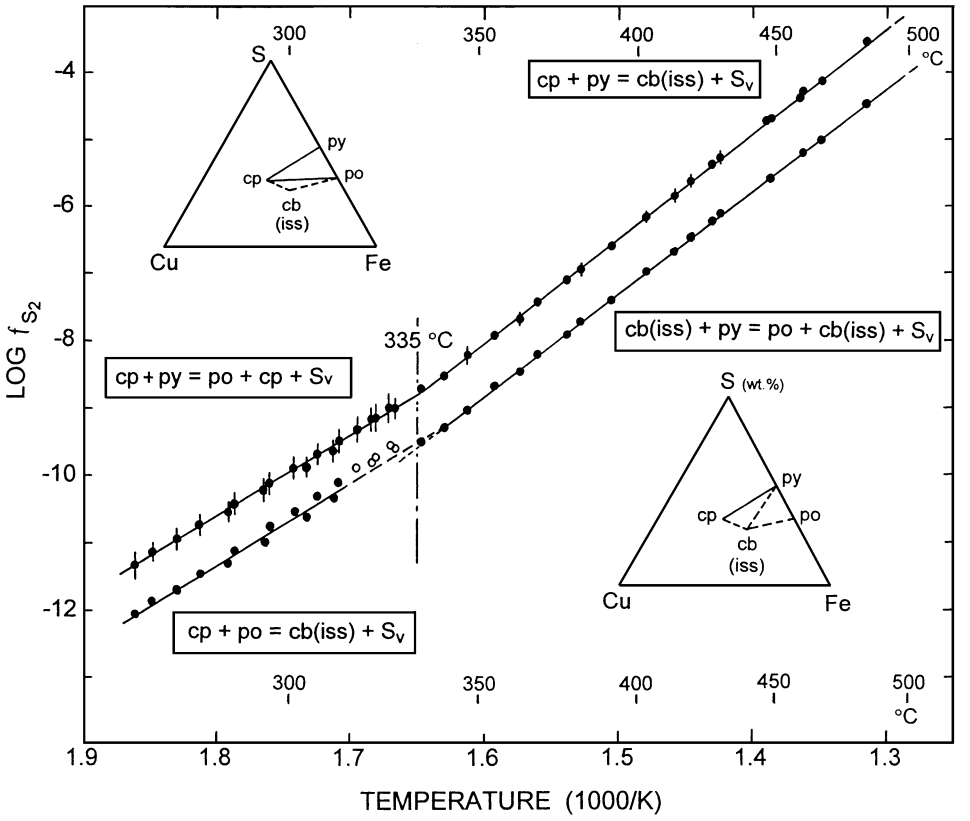

Fig. 4. Sulfur fugacity versus 1000/T plots for a quartet of reactions involving pyrite, pyrrhotite, chalcopyrite and cubanite (iss: intermediate solid solution). Data represented by the empty symbols have been excluded from the regression analyses.

al. (1973b). Uncertainties for the second (i.e., −9,229.0) and third (i.e., 3.76) constants of this equation are estimated to be of the order of ±1%. However, we could have chosen cell equations that link Kiukkola and Wagner's (1957) data with the $\log f^0_{S_2}$ polymerization models of Rickert (1968), Mills (1974) or others, for example. The relative accuracy of these alternative polymerization models can be checked by comparing sulfur fugacities calculated at chosen temperatures for the $4Ag_{(s)}+S_{2(g)}=2Ag_{2+x}S_{(s)}$ (i.e., silver-saturated argentite) reaction where voltage is set at zero in the respective cell equations. Accordingly, our chosen equation yields $\log f_{S_2}$ values of −11.67 and −9.01 units at 325 and 450 °C, respec-

Table 5
Sulfur fugacity measurements for a quartet of reactions involving pyrite, pyrrhotite, chalcopyrite and cubanite (iss)

Measurement details	Temperature (°C)	Temperature 1000/K	Cell voltage (ε, mV±1σ)	Sulfur fugacity $\log f_{S_2}$ (±1σ)	Temperature (°C)	Cell voltage (ε, mV±1σ)	Sulfur vapour $\log f_{S_2}$ (±1σ)
A. Chalcopyrite+pyrite=cubanite (iss)+sulfur (vapor)					*C. Cubanite (iss)+pyrite=cubanite (iss)+pyrrhotite+sulfur (vapor)*		
28—(4/212)/3	488	1.314	177.4±0.8	−3.67±0.02	488	146.9±1.1	−4.48±0.03
27—(3/208)/3	469	1.348	166.8±1.2	−4.15±0.02	469	135.0±1.1	−5.02±0.03
8—(5/86)/3	461	1.362	164.6±2.6	−4.29±0.07	461	131.6±1.0	−5.20±0.02
26—(7/205)/3	460	1.364	162.0±1.4	−4.38±0.02	460	130.1±1.0	−5.25±0.02
25—(7/198)/3	448	1.386	154.8±1.9	−4.71±0.05	448	123.0±0.9	−5.60±0.03
9—(5/91)/3	447	1.389	155.1±2.8	−4.72±0.07	447	123.6±0.8	−5.60±0.02
10—(6/97)/3	429	1.424	142.9±2.9	−5.28±0.08	429	113.3±0.9	−6.13±0.02
24—(7/191)/3	426	1.430	140.4±2.3	−5.39±0.07	426	110.8±0.9	−6.24±0.02
11—(6/103)/3	419	1.446	135.6±2.7	−5.63±0.08	419	107.3±0.8	−6.46±0.02
23—(7/184)/3	413	1.458	131.0±2.3	−5.85±0.06	413	102.5±1.0	−6.69±0.03
12—(6/109)/3	403	1.479	125.1±2.6	−6.16±0.08	403	98.1±0.9	−6.97±0.03
22—(7/177)/3	391	1.505	116.7±2.2	−6.59±0.07	391	90.0±1.0	−7.40±0.03
13—(6/115)/3	390	1.507	116.6±2.5	−6.61±0.08	390	90.8±0.9	−7.39±0.03
14—(6/121)/3	381	1.528	110.3±2.4	−6.95±0.08	381	85.2±0.9	−7.72±0.03
21—(7/170)/3	377	1.538	107.2±2.3	−7.11±0.07	377	81.4±0.9	−7.91±0.03
15—(6/127)/3	368	1.560	102.0±1.8	−7.43±0.06	368	77.6±1.1	−8.20±0.03
20—(7/163)/3	363	1.573	97.3±2.3	−7.67±0.08	363	72.6±0.9	−8.45±0.03
16—(4/131)/3	355	1.592	93.6±2.0	−7.93±0.06	355	70.2±0.9	−8.68±0.03
19—(7/156)/3	347	1.612	89.5±4.8	−8.21±0.16	347	63.9±0.9	−9.04±0.03
18—(6/149)/3	341	1.629	83.8±0.6	−8.53±0.02	341	60.4±0.9	−9.29±0.03
17—(12/143)/3	334	1.646	81.5±0.4	−8.72±0.1	334	57.8±0.9	−9.51±0.03
B. Chalcopyrite+pyrite=pyrrhotite+chalcopyrite+sulfur (vapor)					*D. Chalcopyrite+pyrrhotite=cubanite+sulfur (vapor)*		
17—(12/220)/2	328	1.665	77.2±4.7	−9.01±0.16	–	–	–
1—(107/107)/2	326	1.669	78.8±7.2	−9.00±0.24	–	–	–
2—(6/113)/2	321	1.682	76.7±6.5	−9.16±0.21	–	–	–
16—(14/208)/2	321	1.682	76.6±6.3	−9.16±0.21	–	–	–
3—(6/119)/2	317	1.694	74.8±5.8	−9.31±0.20	–	–	–
4—(6/125)/2	312	1.708	72.7±5.3	−9.50±0.18	312	55.0±1.5	−10.11±0.05
15—(7/194)/2	311	1.711	69.6±5.0	−9.63±0.17	311	49.2±0.8	−10.34±0.03
5—(6/131)/2	307	1.724	70.5±4.9	−9.70±0.17	307	52.8±1.3	−10.31±0.05
14—(7/187)/2	304	1.732	66.9±4.5	−9.89±0.16	304	45.6±0.8	−10.63±0.03
6—(4/135)/2	301	1.741	68.5±4.7	−9.90±0.17	301	50.6±1.3	−10.53±0.05
7—(4/139)/2	295	1.759	66.5±4.4	−10.12±0.16	295	48.2±1.2	−10.77±0.04
13—(7/180)/2	294	1.763	63.9±4.1	−10.24±0.15	294	42.4±0.8	−11.01±0.03
8—(7/146)/2	287	1.786	63.5±4.3	−10.44±0.16	287	44.4±1.1	−11.12±0.04
12—(7/173)/2	286	1.790	61.8±4.0	−10.53±0.14	286	40.6±0.8	−11.30±0.03
9—(6/152)/2	279	1.812	61.0±4.2	−10.73±0.15	279	41.3±1.0	−11.45±0.04
11—(7/166)/2	274	1.829	58.9±4.0	−10.95±0.15	274	38.1±1.0	−11.71±0.04
10—(7/159)/2	268	1.847	57.9±4.0	−11.13±0.16	268	37.8±0.9	−11.88±0.03

Table 6
Sulfur fugacity measurements for the pyrite=pyrrhotite+sulfur (vapor) reaction

Measurement details	Temperature (°C)	Temperature 1000/K	Cell voltage (ε, mV±1σ)	Sulfur fugacity $\log f_{S_2}$ (±1σ)
A-1. Present data above 325 C				
11—(4/151)/4	448	1.387	119.7±0.6	−5.69±0.02
10—(4/147)/4	438	1.406	112.9±0.7	−6.02±0.02
12—(4/155)/4	434	1.415	111.2±1.0	−6.13±0.04
18—(5/190)/4	413	1.457	97.9±1.4	−6.81±0.05
8—(6/137)/4	410	1.464	96.6±1.2	−6.91±0.05
1—(23/23)/4	404	1.478	95.2±1.7	−7.05±0.06
19—(5/195)/4	402	1.480	93.0±1.4	−7.13±0.06
7—(9/131)/4	396	1.494	89.5±1.5	−7.34±0.06
2—(7/30)/4	394	1.498	90.6±1.9	−7.33±0.07
14—(6/166)/4	392	1.503	89.4±1.1	−7.41±0.04
3—(12/42)/3	381	1.528	85.1±2.2	−7.72±0.08
6—(45/122)/4	376	1.541	79.7±1.5	−7.99±0.06
16—(6/178)/4	371	1.554	78.5±1.1	−8.12±0.05
4—(13/55)/4	369	1.556	78.3±2.5	−8.15±0.09
20—(25/221)/4	361	1.576	71.8±1.1	−8.51±0.05
*1—(6/6)/2	351	1.601	64.1±1.2	−8.95±0.04
*2—(21/27)/2	334	1.646	57.3±0.1	−9.53±0.01
*3—(7/34)/2	330	1.658	55.4±0.3	−9.69±0.01
A-2. Data above 325 °C from other sources				
T & B (1964)	742	0.985	–	+0.84±0.15
T & B (1964)	736	0.991	–	+0.69±0.15
T & B (1964)	700	1.028	–	0.00±0.15
T & B (1964)	677	1.052	–	−0.43±0.15
T & B (1964)	648	1.086	–	−1.00±0.15
T & B (1964)	602	1.143	–	−1.95±0.15
T & B (1964)	599	1.147	–	−2.00±0.15
T & B (1964)	555	1.208	–	−3.00±0.15
T & B (1964)	514	1.270	–	−4.00±0.15
K & S (1979)	460	1.364	–	−5.41±0.10
T & B (1964)	443	1.396	–	−6.00±0.15
Schn (1973)	438	1.406	–	−5.93±0.25
K & S (1979)	413	1.458	–	−6.70±0.10
Schn (1973)	401	1.484	–	−7.05±0.21
B. Data between 325 °C and the ~291 °C inflection point				
Schn (1973)	324	1.675	–	−10.01±0.24
*4—(5/49)/2	321	1.683	52.2±0.5	−10.01±0.02
*5—(9/58)/2	317	1.696	49.7±1.3	−10.19±0.04
*6—(12/70)/3	307	1.723	42.3±3.7	−10.67±0.13
*7—(7/77)/3	302	1.739	39.9±3.9	−10.90±0.14
*8—(11/88)/3	297	1.753	38.1±3.4	−11.07±0.12
*9—(10/98)/3	294	1.764	36.1±3.6	−11.23±0.12
C. Data below the ~291 °C inflection point				
*11—(4/109)/3	286	1.788	32.9±3.5	−11.56±0.14
*12—(10/119)/3	282	1.802	30.9±3.0	−11.75±0.11
*13—(14/133)/3	277	1.816	28.8±2.9	−11.95±0.11
*14—(15/148)/3	272	1.834	27.2±3.7	−12.17±0.14
*15—(7/155)/3	268	1.848	25.1±4.1	−12.36±0.15
C. Data below the ~291 °C inflection point				
*16—(10/165)/3	265	1.860	23.0±3.9	−12.54±0.15
*17—(4/179)/3	261	1.871	21.8±4.1	−12.69±0.15
*18—(9/178)/3	257	1.888	19.4±4.5	−12.93±0.17
*19—(16/194)/3	252	1.903	17.7±5.3	−13.13±0.20
*20—(29/223)/3	247	1.923	16.5±6.0	−13.35±0.23
*21—(20/243)/3	243	1.938	14.1±5.4	−13.58±0.21

In panel A-2, the smoothed data of Toulmin and Barton (1964) (T & B, 1964) is reported directly from their Table 5. A conservative uncertainty of ±0.15 log units is presently assigned to this data set. The sulfur fugacities given for Schneeberg (1973) (Schn, 1973) and Kissin and Scott (1979) (K & S, 1979) have been recalculated using the present cell equation. A second set of experiments (marked by*) was used to obtain data for temperatures ≤351 °C.

tively. These agree to within 0.05 to 0.07 log units for sulfur fugacity calculated at the same temperatures using the free energy data reported in Kubaschewski et al. (1967). On the other hand, cell equations using the sulfur polymerization models of Rickert (1968) and Mills (1974) yield sulfur fugacities that are higher by 0.21 and 0.25 log units. The *anticipated* accuracy is ±0.1–0.15 log units using the present cell equation in conjunction with Schneeberg-type cells. This uncertainty is notional because individual cells of the Schneeberg-type cannot be calibrated. It is therefore essential to use multiple cells in any study.

Cell voltage measurements are included with our results. The 1σ error values provided with our voltage and sulfur fugacity data are for precision directly related to the cell measurements. It should be noted that the sulfur fugacity data from Schneeberg (1973) and Kissin and Scott (1979) have been recalculated using the cell equation above.

4.3. Sulfur fugacity for reactions involving minerals of the Cu–Fe–S system

4.3.1. The Id+py=bn+S reaction

This reaction was investigated between 187 and 448 °C over a period of 127 days. The data presented in Table 2 and shown plotted in Fig. 3 indicate an inflection at ~221 °C. This was not detected by Schneeberg (1973). Furthermore, a dashed line that is displaced to higher values of sulfur fugacity represents his residual data above the inflection point.

Table 3 presents regression equations for these reactions and also others that follow.

The dashed extrapolation of our higher temperature data intersects the sulfur condensation curve at approximately 485 °C, or 16 °C lower than the 501 °C invariant point determined by Roseboom and Kullerud (1958) using differential thermal analysis. This represents reasonable agreement when allowance is made

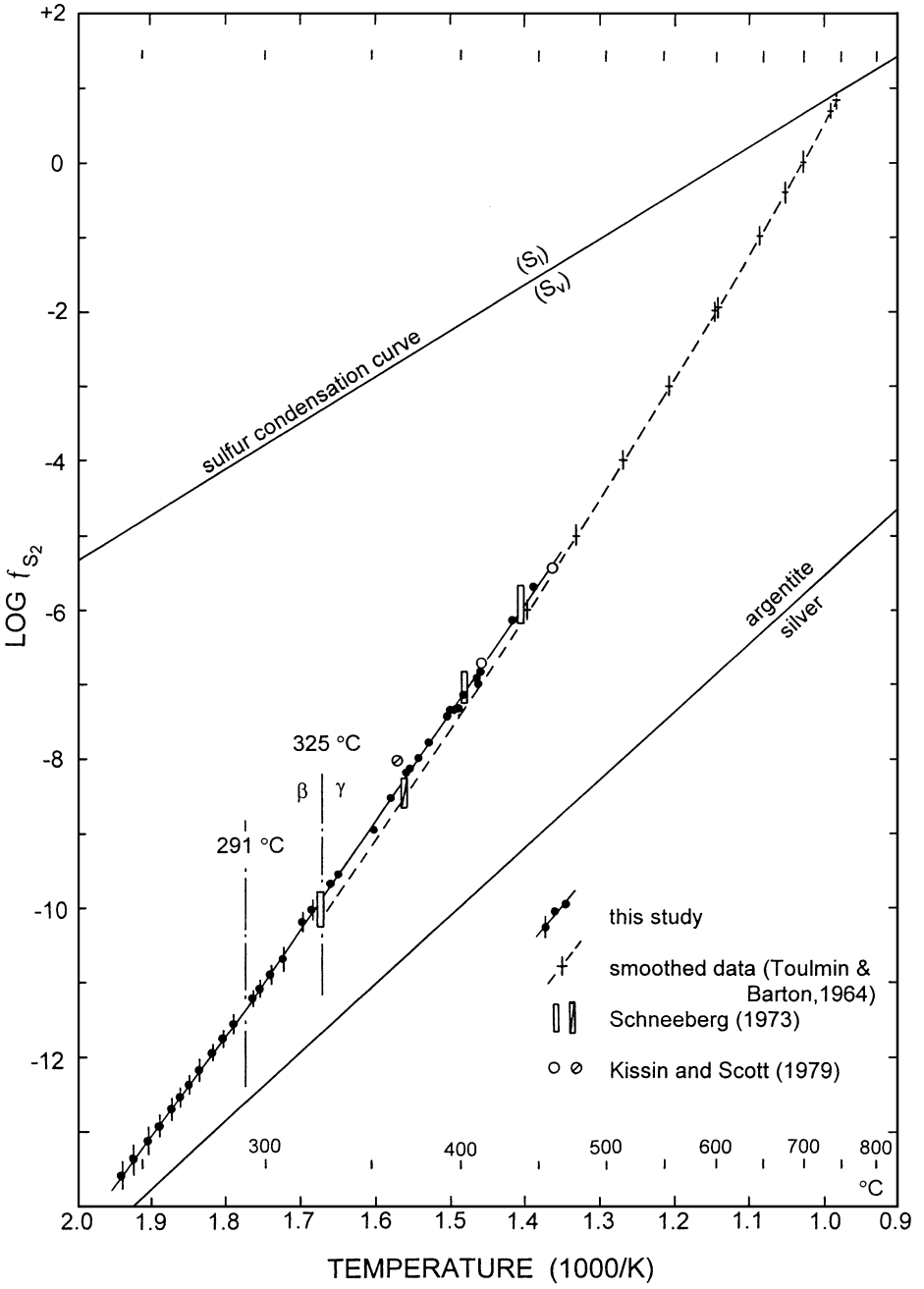

Fig. 5. Sulfur fugacity versus 1000/*T* plot for the pyrite = pyrrhotite + sulfur (vapor) reaction. The open symbols with diagonal slashes indicate data that have been excluded from the regression analyses.

for the relatively small angular separation in slopes between the intersecting curves. However, the extrapolation of Schneeberg's higher temperature data intersects the sulfur condensation curve around 440 °C, close to the ~434 °C (Roseboom and Kullerud, 1958) invariant point for the py+ cv=id+ S (liquid) reaction.

4.3.2. The bn+py=cp+S reaction

This reaction has been investigated in two sets of experiments at temperatures between 206 and 485 °C for a total of 290 days. The results are given in Table 4 and are shown plotted in Fig. 3.

The data reveal a ~237 °C inflection point that has not been identified by Schneeberg (1973). However, his data above the inflection point show excellent agreement with the present higher temperature data. Barton and Toulmin's (1964b) four data obtained using the electrum tarnish method also show excellent agreement.

4.3.3. Quartet of reactions involving the minerals cp, cb(iss), py and po

Pyrite, pyrrhotite, chalcopyrite and cubanite (iss) form equilibrium associations in a relatively iron-rich and sulfur-poor region of the Cu–Fe–S system at temperatures below 532 °C (Barton, 1973). Cubanite is a distinct mineral at low temperatures but forms an extensive solid solution at intermediate and higher temperatures (Merwin and Lombard, 1937; Cabri, 1973; Barton, 1973). It is synonymous with *intermediate solid solution*, or iss, which has a cubic sphalerite-type structure (Yund and Kullerud, 1966). This distinguishes it from the chalcopyrite solid solution that has a tetragonal structure. The iss suffix is used in this study to denote that cubanite is an extensive and structurally distinctive solid solution at higher temperatures.

A pyrite–cubanite (iss) tie line exists from 532 to 334 °C, but is replaced by a pyrrhotite–chalcopyrite tie line below the 334 °C invariant temperature. In compositional diagrams the pyrite–cubanite (iss) tie line is shared by two reactions, namely, the cp+py=cb (iss)+S reaction at higher sulfur fugacity and the cb (iss)+py=po+cb (iss)+S reaction at lower sulfur fugacity. The reactions cp+py=po+cp+S and cp+po=cb (iss)+S share the pyrrhotite–chalcopyrite tie line below the invariant temperature, with the cp+py=po+cp+S reaction corresponding to higher sulfur fugacity. These phase relationships are illustrated schematically in the compositional diagrams that are shown as insets in Fig. 4.

Experiments involving the two higher temperature reactions were carried out at temperatures between 341 and 488 °C for 208 days. The two lower temperature reactions were studied between 268 and 312 °C over 194 days. The results are presented in Table 5(A–C) and are plotted in Fig. 4. The intersection of the regression lines (Table 3) for the upper set of reactions

Table 7
Sulfur fugacity measurements for pyrrhotites

Measurement details	Temperature (°C)	Temperature 1000/K	Cell voltages (ε, mV±1σ)	Sulfur fugacity $\log f_{S_2}$ (±1σ)
A. Data for pyrrhotites with N_{FeS}=0.9464±0.0025				
10—(6/89)/2	422	1.439	74.1±7.2	−7.37±0.21
1—(17/17)/2	404	1.477	75.2±12.5	−7.64±0.37
9—(7/83)/2	402	1.482	69.7±8.7	−7.84±0.26
2—(8/25)/2	388	1.512	69.8±12.2	−8.07±0.37
3—(34/59)/2	349	1.608	57.1±12.6	−9.23±0.41
4—(3/62)/2	330	1.659	51.7±12.6	−9.83±0.42
B. Data for pyrrhotites with N_{FeS}=0.9480±0.003				
12—(4/155)/2	434	1.415	74.5±5.4	−7.18±0.15
13—(5/160)/2	414	1.456	69.3±4.9	−7.65±0.13
19—(5/195)/2	402	1.480	63.2±7.1	−8.02±0.21
15—(6/172)/2	394	1.499	60.4±3.8	−8.25±0.12
14—(6/166)/2	392	1.503	63.7±4.1	−8.18±0.13
3—(12/42)/2	381	1.528	65.1±1.9	−8.34±0.06
16—(6/178)/2	371	1.554	57.8±3.6	−8.77±0.11
4—(13/55)/2	369	1.556	61.3±2.0	−8.69±0.06
20—(25/221)/2	361	1.576	53.3±4.9	−9.09±0.15
17—(7/185)/2	355	1.591	53.6±3.4	−9.21±0.15
C. Data for pyrrhotites with N_{FeS}=0.9545±0.003				
11—(6/94)/2	440	1.403	50.9±5.7	−7.75±0.16
10—(6/89)/2	422	1.439	47.6±4.8	−8.14±0.14
1—(17/17)/2	404	1.477	47.2±5.9	−8.47±0.18
9—(7/83)/2	402	1.482	43.9±4.7	−8.61±0.14
2—(8/25)/2	388	1.512	41.8±4.9	−8.93±0.15
8—(7/76)/2	376	1.542	37.9±4.7	−9.29±0.14
3—(34/59)/2	349	1.608	30.5±4.3	−10.09±0.14
7—(2/69)/2	339	1.635	27.8±4.5	−10.42±0.15
4—(3/62)/2	330	1.659	25.2±4.5	−10.71±0.16
5—(3/65)/2	313	1.707	20.8±4.8	−11.28±0.16
6—(2/67)/2	299	1.747	17.2±5.1	−11.76±0.18
D. Data for pyrrhotites with N_{FeS}=0.9625±0.0005				
12—(5/99)/2	456	1.372	21.3±5.5	−8.32±0.15
11—(6/94)/2	440	1.403	18.4±5.6	−8.67±0.16
10—(6/89)/2	422	1.439	14.9±5.8	−9.09±0.17
1—(17/17)/2	404	1.477	12.2±5.4	−9.52±0.16
9—(7/83)/2	402	1.482	10.1±6.6	−9.62±0.19
2—(8/25)/2	388	1.512	7.1±5.2	−9.98±0.16

is precisely located at 335 °C. The lower pair of reactions intersect around 340 °C, and the py=po+ S reaction line (not shown) intersects the cp+po=cb(iss)+S reaction line near 330 °C. Together, these intercepts approximately bracket the 335 °C invariant point. Our invariant temperature, where four mineral phases coexist with vapor, is in excellent agreement with the 334±17 °C temperature determined by Yund and Kullerud (1966) using differential thermal analysis.

4.4. The py=po+S reaction

This reaction was investigated in two sets of experiments spanning a temperature interval from 243 to 448 °C. The higher temperature experiments were conducted for 221 days and the lower temperature set for 243 days. The results are presented in Table 6(A–C) and are shown plotted in Fig. 5. The data of Schneeberg (1973) and of Kissin and Scott (1979), together with a dashed curve representing the smoothed data of Toulmin and Barton (1964) are also indicated.

The present results reveal an inflection at 291 °C. A subtle inflection may also occur at 325 °C, as Toulmin and Barton (1964) suggest in their Figs. 3 and 4. This is not confirmed by our results.

For temperatures above 325 °C, the present data show excellent agreement with the three data points from Schneeberg (1973) and two from Kissin and Scott (1979). The dashed curve representing smoothed data from Toulmin and Barton (1964) lies ~0.3 log units lower at 325 °C and ~0.1 log units lower at 450 °C, thus supporting criticisms by some researchers (e.g., Scott and Barnes, 1971; Kissin and Scott, 1979; Barker and Parkes, 1986) that the data of Toulmin and Barton (1964) occur at too low fugacities in this $\log f_{S_2}-T$ region.

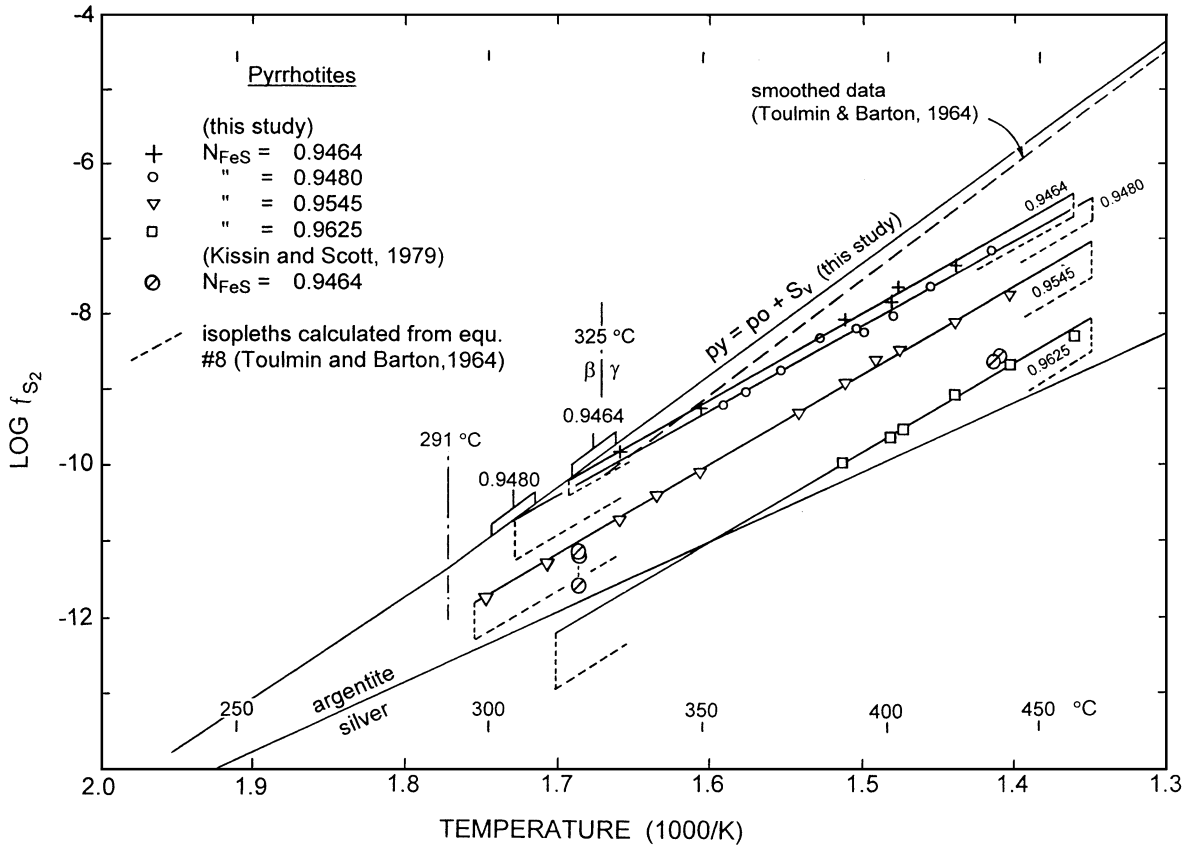

Fig. 6. Sulfur fugacity versus 1000/T plot for pyrrhotites.

4.5. Experiments with pyrrhotite

The results of two sets of experiments involving four pyrrhotite compositions are presented in Table 7 and are shown plotted in Fig. 6. Kissin and Scott's (1979) sulfur fugacity measurements for a single crystal of NC-type pyrrhotite (N_{FeS}=0.9464 (or 47.32 at.% Fe)) are also plotted, together with the present py=po+ S reaction line (i.e., Eq. (5b), Table 3) and a dashed curve representing Toulmin and Barton's (1964) smoothed data for the same reaction.

Pyrrhotites with the compositions N_{FeS}=0.9464 and 0.9480 occur on the pyrite–pyrrhotite solvus. Their locations were interpolated from independent temperature–composition data sourced from Arnold (1962) and Schneeberg (1973).

Toulmin and Barton's (1964) Eq. (8) was used to calculate sulfur fugacity for the respective pyrrhotite compositions at chosen temperatures. Corresponding isopleths are shown as lightly dashed lines extending beyond the arbitrary 325 to 450 °C reference interval. The extrapolation of the regression isopleth for the most sulfur-rich pyrrhotite (i.e., N_{FeS}=0.9464; Eq. (6a), Table 3) used in the present study intersects the pyrite–pyrrhotite solvus slightly below the equivalent pyrrhotite composition on the solvus. However, the intersection of the isopleth for the slightly more iron-rich pyrrhotite (i.e., N_{FeS}=0.9480; Eq. (6b), Table 3) shows excellent agreement with its solvus equivalent. The two remaining pyrrhotites (i.e., N_{FeS}=0.9545 and 0.9625) occur at lower fugacities and do not intersect the pyrite–pyrrhotite solvus in the temperature interval shown.

Kissin and Scott's (1979) measurements with a single crystal of pyrrhotite of precisely known initial composition (i.e., N_{FeS}=0.9464) are displaced to sulfur fugacity values that are well below the calculated equivalents. Furthermore, the slope of their experimental isopleth is considerably lower than the slopes of calculated isopleths nearby.

5. Discussion

The present data for the sulfur condensation curve are displaced to lower voltages but have a very similar slope to Kiukkola and Wagner's (1957) curve. However, a displacement of approximately 1 mV is larger than was anticipated and suggests a systematic error (or errors). A comparison of the experimental methods reveals important differences in the designs of the measurement cells. The present method involved evacuated cells with relatively large surface areas of liquid sulfur in direct communication with large vapor spaces. Post-experiment inspection of the cells suggested contamination of the sulfur by gaseous iodine, although this was not quantified. Additionally, the relatively small volumes of AgI electrolyte in the cells were strongly discolored at the end of the experiments, suggesting possible formation of silver sulfide iodide. On the other hand, Kiukkola and Wagner's (1957) method involved a large reservoir of solid AgI electrolyte in which the silver electrode was deeply embedded, as well as a relatively small area for electrolyte–sulfur exchange. These factors should have kept cross-contamination to a minimum, and may explain the ~0.4% difference between the voltages for the two methods.

The extrapolation of present data for the id+ py=bn+S reaction shows reasonable agreement (i.e., 485 °C) with the 501 °C invariant temperature determined by Roseboom and Kullerud (1958) using differential thermal analysis. On the other hand, an extrapolation of Schneeberg's (1973) data intersects the sulfur condensation curve at ~440 °C, some 35 °C lower than the present data. It thus appears that Schneeberg's (1973) data occur at excessively high values of sulfur fugacity. However, the difference appears to be systematically related, and this could reflect some problem associated with the sulfide mixture that Schneeberg (1973) used in his experiments. Perhaps pyrite did not fully participate in the reaction and/or his mixture may have contained covellite, which should not have been present. If the latter were true, this may account for the close agreement between his ~440 °C extrapolation temperature and the 434 °C invariant temperature for the cv+ py=id+ S (liquid) reaction determined by Roseboom and Kullerud (1958). Schneeberg's (1973) data for the cv+py=id+S reaction intersects the sulfur condensation curve around 380 °C, or approximately 55 °C lower than the expected temperature. Hence, Schneeberg's (1973) data for this reaction also appear to be in error.

The py+id=bn (sulfur-rich)+S and py+bn (sulfur-depleted)=cp+S reactions share bn+py tie lines from a

maximum of ~532 °C (Barton, 1973) down to <220 °C where covellite and pyrite substitute for idaite. Barton and Skinner (1979) calculated a probable temperature of 227±50 °C for this invariant point. The extreme positions of py+bn tie lines are represented by an extensive pyrite+ bornite stability region in $\log f_{S_{2(T)}} - 1000/T$ space, as shown in Fig. 7. The ~221 and ~237 °C inflections mark structural changes for the sulfur-rich (high) and sulfur-depleted extremes of the bornite solid solution. A non-quenchable face-centered cubic form of bornite solid solution is stable above these temperatures and the tetragonal form is stable below. Morimoto and Kullerud (1961) proposed a single inversion temperature at 228±5 °C. However, Pankratz and King (1970) and Sugaki and Shima (1965) foreshadowed dual inversion temperatures (i.e., ~200 and ~270 °C).

The present study suggests that the py+bn=cp+S reaction curve is essentially linear until it reaches the ~532 °C (Barton, 1973) invariant point where the

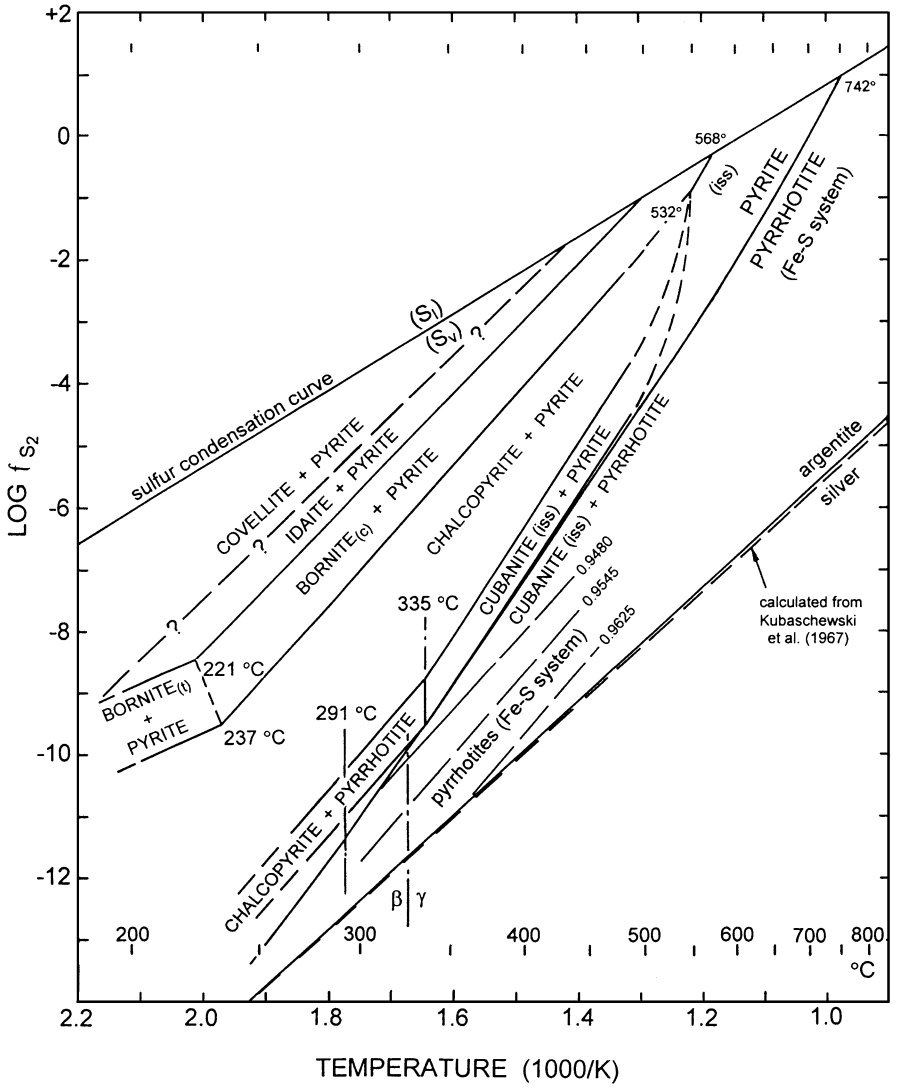

Fig. 7. Log f_{S_2} versus $1000/T$ map for selected reactions in the Cu–Fe–S and Fe–S systems.

sulfur fugacity is approximately −0.8 log units (Merwin and Lombard, 1937). The bn+py=iss (or intermediate solid solution)+S reaction commences at the ~532 °C invariant point and intersects the sulfur condensation curve at ~568 °C where the sulfur fugacity is approximately −0.36 log units (Roseboom and Kullerud, 1958).

The presently investigated cp+py=cb (iss)+S and cb (iss)+py=cb (iss)+po+S reactions appear to terminate at the ~532 °C invariant point. Our data suggest that both reactions are essentially linear between ~335 and ~480 °C. Hence, moderately high rates of increase in sulfur fugacity are implied for the intervening ~490 to ~532 °C temperature interval, as suggested in Fig. 7.

The 335 °C invariant temperature is precisely fixed in the present study and confirms the 334±17 °C determination by Yund and Kullerud (1966). At this temperature, cp, py, cb (iss) and po should coexist in equilibrium with vapor at a unique sulfur fugacity. However, our data suggest *two* sulfur fugacities with a difference of approximately one log unit between them. This apparent paradox is only possible where true compositional equilibrium has not been achieved between the two sets of shared mineral phases. This is not surprising because reaction rates are slow and intrinsic sulfur fugacities are low in this iron-rich portion of the Cu–Fe–S system (Cabri, 1973). A symmetry of behavior suggests that the higher sulfur fugacity at the invariant temperature corresponds to that of a cubanite–chalcopyrite tie line (i.e., ~−8.8 log units), in the same way that the lower sulfur fugacity (i.e., ~−9.6 log units) approximates that of the py=po+S reaction (Fe–S system) at the same temperature.

The present data for the py=po+S reaction show excellent agreement with the data of Schneeberg (1973) and of Kissin and Scott (1979). This collective data indicates that the pyrite–pyrrhotite reaction is essentially linear between 291 and 460 °C, but occurs at slightly higher sulfur fugacities than Toulmin and Barton's smoothed data for the 325–460 °C interval. However, overlap of these data sets occurs around 480 °C. The smoothed data of Toulmin and Barton (1964) are the best available at temperatures between ~500 and the 742±1 °C (Barton, 1969) invariant temperature (i.e., Fe–S system). The latter is lowered by only a few degrees in the Cu–Fe–S system (Roseboom and Kullerud, 1958). It is reasonable, therefore, to combine the present data with Toulmin and Barton's (1964) higher temperature data. The equation (i.e., 5e, Table 3)

$$\log f_{S_2} = 19.007 - 2.2119 \times 10^4 (1/T) + 1.8602 \times 10^6 (1/T)^2 \quad (4)$$

is thus obtained for the 294–742 °C temperature range. An R^2 value of 0.9997 indicates a good fit to the combined data.

The temperatures 325 and ~291 °C are flagged in Figs. 5–7. The 325 °C temperature identifies the β to γ magnetic transition (Haraldsen, 1937) that occurs in disordered (1C) hexagonal pyrrhotite that is relevant to the sphalerite geobarometer. Kubaschewski et al. (1967) report a thermal change of 120 cal/mol for this transition. The present data do not indicate an inflection, although one can be anticipated. On the other hand, a definite inflection was found at ~291 °C, and this may correspond to a discontinuity that was reported by Lusk et al. (1993). It is noteworthy that this inflection is contained within the ~308 to ~262 °C stability interval that has been proposed by Kissin and Scott (1982) for the MC superstructure type in hexagonal pyrrhotite. This and other superstructure types were identified and named from single crystal X-ray studies by Nakazawa and Morimoto (1970) and Nakazawa (1971). The presently determined ~291 °C inflection may locate the real boundary between the disordered 1C and the ordered MC types.

The pyrrhotites in the present study are displaced to higher sulfur fugacities than equivalent isopleths calculated from Toulmin and Barton's (1964) Eq. (8). A comparison reveals two notable features. The first is the excellent agreement between the slopes of the measured and calculated isopleth sets that diverge with a lowering of both temperature and sulfur fugacity. The second is a systematic and increasing displacement to lower sulfur fungacities for the calculated isopleths that correspond to the N_{FeS}=0.9480, 0.9545 and 0.9625 compositions. The respective displacements increase in this order from ~0.5 to ~0.9 log units at 325 °C, and from ~0.4 to ~0.7 log units at 450 °C. The displacements for Kissin and Scott's (1979) novel experiments involving pyrrhotite crystals in a heated X-ray goniometer are larger, but in the opposite direction. It is evident that equilibrium sulfur

fugacity values were not attained in these experiments. A too small pyrrhotite sample mass in relation to the experimental vapor volume and/or the mass of the silver sulfide electrode could have been important contributing factors.

Toulmin and Barton (1964) estimated a total error of ±0.35 log units for sulfur fugacity in relation to carefully determined pyrrhotite compositions (i.e., ±0.002 in N_{FeS}) obtained by the X-ray method. In the present study we report a maximum compositional uncertainty of ±0.003 for our pyrrhotites, a maximum uncertainty of 0.15 log units for the accuracy of our cell equation, and an average error of 0.15 log units for cell measurement with the N_{FeS}=0.9545 pyrrhotite as an example. From these individual errors we obtain estimates of maximum total error of ±0.50 log units at 325 °C, and ±0.4 log units at 450 °C. Consequently, there is an overlap of errors associated with our measured pyrrhotites and the calculated values from Toulmin and Barton (1964) using the electrum tarnish method.

Differences in sulfur fugacity determinations between the present study and those of Barton and Toulmin (1964b) and Toulmin and Barton (1964) increase systematically with both decreasing temperature and decreasing sulfur fugacity. Excellent agreement is obtained for the py+bn=cp+S reaction at higher sulfur fugacity. Minor disagreement is evident for the py=po+S reaction, and serious disagreement is evident for pyrrhotites. The differences in sulfur fugacity are also accompanied by a progressive divergence in slopes for the respective reactions. These shared consistencies suggest that equilibrium conditions were achieved and measured in the above-mentioned studies. The cause of the disagreements is attributed to the accuracy of the fundamental parameters that are used in determining sulfur fugacity by the two methods. There are also some calibration difficulties that are unique to the electrum tarnish method (Barton and Toulmin, 1964a).

Barton and Toulmin (1964a) chose the fundamental data of West (1950) and Braune et al. (1951) in relation to $\log f_{S_{2(T)}}$ quantities, data from White et al. (1957) pertaining to electrum alloys, and data from Richardson and Jeffes (1952) in relation to the $Ag_2S_{(s)}=Ag_{(s)}+S_{2(g)}$ reaction. For the calibration of electrum tarnish curves they claim an uncertainty of ±0.13 $\log f_{S_2}$ units. In the present study we use the ε^0 data of Kiukkola and Wagner (1957) in conjunction with that of Rau et al. (1973b) in obtaining an estimated calibration error of ±0.11–0.15 log units for sulfur fugacity at temperatures between 200 and 500 °C. This suggests reasonable agreement with the calibration error claimed for the electrum tarnish method.

The errors of measurement must also be taken into account when applying these methods. The former include the *recognition* of equilibrium conditions and their determination through measurement. With the electrochemical method both the recognition of equilibrium and its measurement are straight forward, thus yielding measurement precisions that are commonly better than ±0.05 log units where temperatures and fungacities are high, and reducing to average precisions of ~±0.15 log units for reactions where sulfur fugacity is intrinsically low. On the other hand, measurement errors are commonly large for the electrum tarnish method. Barton and Toulmin (1964a) acknowledged that the largest source of potential error stems from the *uncertainty of decision* in visually estimating the temperatures at which tarnishes appear and disappear. This recognition yields pairs of temperatures with variable differences between them. Tight intervals range from 5 to 10 °C, but others range up to a few tens of degrees (Barton and Toulmin, 1964a). Toulmin and Barton's (1964) 367 °C datum for the pyrite–pyrrhotite reaction serves as an example. A 17 °C temperature interval applies, and this equates with a potential measurement error of ±0.28 log units, and a total uncertainty of ±0.31 log units. For the same reaction at similar temperatures, our cells indicate measurement errors of ±0.05–0.09 log units, and a total uncertainty ±0.17 log units.

6. Conclusions

The electrochemical method for measuring sulfur fugacity is a very powerful tool. The method's greatest strengths are its high sensitivity and its ability to precisely monitor progress in approaching equilibrium for sulfide reactions, including those that have unquenchable phases. The method does have some negative aspects, however. The fabrication of Schneeberg-type cells requires careful technique and some basic glass blowing skills. Nor can individual cells be calibrated, but this is not a serious concern in routine

measurement where multiple cells are used. Indeed, this approach is essential because it compensates for cell fragility, occasional leakage, or simply erratic behavior that cannot be explained.

In the present study we have re-measured the sulfur fugacity for reactions previously studied, and explored several additional reactions for the first time. The present results suggest that Schneeberg's (1973) data for the id+py=bn+S reaction appear to be in error, perhaps due to a sulfide mixture problem, and that inflections occur for the id+py=bn+S and bn+py=cp+S reactions at lower temperatures. Aside from these disagreements, there is excellent agreement with Schneeberg's (1973) data for the py=po+S reaction and for the bn+py=cp+S reaction above the inflection point. For the latter reaction there is also excellent agreement with Barton and Toulmin's (1964b) few data that were obtained using the electrum tarnish method.

The present results show moderate disagreement with Toulmin and Barton's (1964) data for the py=po+S reaction, particularly at lower temperatures, and increasingly serious disagreement for pyrrhotites as sulfur content and temperature decrease. Systematic behavior of this kind can be expected where different parameters are used in calibration equations, and/or where measurement is difficult under certain conditions. Indeed practical difficulties in measurement are greatest for the electrum tarnish method at low temperatures and at low sulfur fungacity. In spite of these difficulties, the data of Barton and Toulmin (1964b) and Toulmin and Barton (1964) appear to the best that can be obtained using a method that is tedious and requires great care in its application.

The inflections obtained for the py+id=bn+S and py+bn=cp+S reactions at lower temperatures represent substantial refinements in our knowledge of a moderately sulfur-rich portion of the Cu–Fe–S system. The former are interpreted as structural (i.e., cubic to tetragonal (low temperature)) inversions for sulfur-rich and sulfur-poor bornites, respectively. The inversion of the high bornite associated with the py+id=bn+S reaction initiates the eventual disappearance of idaite in favor of covellite and pyrite at lower temperatures. The new data obtained for a quartet of reactions sharing the minerals py, po, cp and cb (iss) confirms an invariant temperature at ~335 °C, only 10 °C higher than the magnetic transition for hexagonal pyrrhotite in the Fe–S system. Perhaps this magnetic transition occurs at higher temperatures in the Cu–Fe–S system and, in turn, may influence the tie line switch at the 335 °C invariant temperature. The ~291 °C inflection point for the pyrite–pyrrhotite reaction needs further investigation because it may locate the boundary between the 1C and MC structural types in hexagonal pyrrhotite.

Acknowledgements

It is a pleasure to acknowledge the assistance of Dr. T. E. Freeman, Department of Physics, Macquarie University, for his help with data analysis. Dr. D.W. Durney, Department of Earth and Planetary Sciences, and Professor A. J. Pitman, Department of Physical Geography, are thanked for allowing J.L. to share their laboratory facilities over the past 2 years. The use of equipment in the Division of Exploration Geosciences, C.S.I.R.O., North Ryde, is gratefully acknowledged. Special thanks are due to G.W. Hansen and J.J. Davis of this Division for their friendly assistance over many years. Finally, we are grateful to the Macquarie University Research Committee for providing special funding that has allowed this project to be completed. **[EO]**

References

Arnold, R.G., 1962. Equilibrium relations between pyrrhotite and pyrite from 325° to 743 °C. Econ. Geol. 57, 72–90.

Barker, W.W., Parks, T.C., 1986. The thermodynamic properties of pyrrhotite and pyrite; A re-evaluation. Geochim. Cosmochim. Acta 50, 2185–2194.

Barton Jr., P.B., 1969. Thermochemical study of the system Fe–As–S. Geochim. Cosmochim. Acta. 33, 841–857.

Barton Jr., P.B., 1973. Solid solutions in the system Cu–Fe–S: Part I. The Cu–S and Cu–Fe–S joints. Econ. Geol. 68, 455–465.

Barton Jr., P.B., Skinner, B.J. 1979. Sulfide mineral stabilities. In: Barnes, H.L. (Ed.), Geochemistry of hydrothermal ore deposits Wiley, New York.

Barton Jr., P.B., Toulmin III, P. 1964a. The electrum tarnish method for the determination of the fugacity of sulfur in sulfide systems. Geochim. Cosmochim. Acta. 28, 619–640.

Barton Jr., P.B., Toulmin III, P. 1964b. Experimental determination of the reaction chalcopyrite+sulfur=pyrite+bornite from 350 to 500 °C. Econ. Geol. 59, 747–752.

Braune, H., Peter, S., Nevelling, V., 1951. Die Dissoziation des Schwefeldampfes. Z. Naturforsch. 62, 32–37.

Browner, E.R. 1987. A thermodynamic and structural study of the iron–nickel sulfide system. Unpublished PhD thesis, Univ. Western Australia.

Cabri, L.J., 1973. New data on phase relations in the Cu–Fe–S system. Econ. Geol. 68, 443–454.

Czamanske, G.K., 1974. The FeS content of sphalerite along the chalcopyrite–pyrite–bornite sulfur fugacity buffer. Econ. Geol. 69, 1328–1334.

Haraldsen, H., 1937. Eine thermomagnetische untersuchung der umwandlungen im Troilit–Pyrrhotin–Gebiet des Eisen–Schwefel–Systems 2. Anerg. Chem. 23, 78–96.

Hutchison, M.N., Scott, S.D., 1981. Sphalerite geobarometry in the Cu–Fe–S system. Econ. Geol. 76, 143–153.

Kissin, S.A., Scott, S.D., 1979. Device for measurement of sulfur fugacity mountable on the precession camera. Am. Mineral. 64, 1306–1310.

Kissin, S.A., Scott, S.D., 1982. Phase relations involving pyrrhotite below 350 °C. Econ. Geol. 77, 1739–1754.

Kiukkola, K., Wagner, C., 1957. Measurements on galvanic cells involving solid electrolytes. J. Electrochem. Soc. 118, 420–425.

Kojima, S., Sugaki, A., 1985. Phase relations in the Cu–Fe–Zn–S system between 500° and 350 °C under hydrothermal conditions. Econ. Geol. 80, 158–171.

Kubaschewski, O., Evans, E.L., Alcock, C.B., 1967. Metallurgical Thermochemistry, 4th ed. Pergamon, New York.

Lusk, J., 1989. An electrochemical method for determining equilibration temperatures for sulfide minerals. Econ. Geol. 84, 1663–1670.

Lusk, J., Ford, C.E., 1978. Experimental extension of the sphalerite geobarometer to 10 kbar. Am. Mineral. 63, 516–519.

Lusk, J., Scott, S.D., Ford, C.E., 1993. Phase relations in the Fe–Zn–S system to 5 Kbars and temperatures between 325° and 150 °C. Econ. Geol. 88, 1880–1903.

Merwin, H.E., Lombard, R.H., 1937. The system, Cu–Fe–S. Econ. Geol. 32, 203–284.

Mills, K.C., 1974. Thermochemical data for inorganic sulphides, selenides and tellurides. Butlerworths, London.

Morimoto, N., Kullerud, G., 1961. Polymorphism in bornite. Am. Mineral. 46, 1270–1283.

Mukaiyama, H., Izawa, E., 1970. Phase relations in the Cu–Fe–S system, the copper–deficient part. In: Tatsumi, T. (Ed.), Volcanism and Ore Genesis. Tokyo Univ. Press, Tokyo.

Nakazawa, H., 1971. Phase relations and superstructures of pyrrhotite, $Fe_{1-x}S$. Mater. Res. Bull. 6, 345–358.

Nakazawa, H., Morimoto, N., 1970. Pyrrhotite phase relations below 320 °C. Jpn. Acad. Proc. 46, 678–683.

Pankratz, L.B., King, E.G., 1970. High-temperature enthalpies and entropies of chalcopyrite and bornite. U. S. Bur. Mines, Rep. Invest. 7435.

Rau, H., 1974. Defect equilibria in silver sulfide. J. Phys. Chem. Solids. 35, 1553–1559.

Rau, H., Kutty, T.R.N., Guedes de Carvalo, J.R.F., 1973a. High temperature saturated vapor pressure of sulfur and the estimation of its critical qualities. J. Chem. Thermodyn. 5, 291–302.

Rau, H., Kutty, T.R.N., Guedes de Carvalo, J.R.F., 1973b. Thermodynamics of sulfur vapor. J. Chem. Thermodyn. 5, 833–844.

Reuter, B., Hardel, K., 1965. Silbersulfidbromid Ag_3SBr und silbersulfidiodid Ag_3SI: 1. Darstellung, eigenschaften und phasenverhaltnisse von Ag_3SBr und Ag_3SI. Z. Anorg. Allg. Chem. 340, 158–167.

Rheinhold, H., 1934. Uber die Bestimmung der Buldungsaffinitat eds silbersulfids (-Selinids-Telurids) durch Elektrometrische Messungen an festen Ketten. Z. Elektrochem. 40, 361–365.

Richardson, F.D., Jeffes, J.H.E., 1952. The thermodynamics of substances of interest in iron and steelmaking: III. Sulfides. J. Iron Steel Inst. 171, 165–175.

Rickert, H., 1968. Kinetic measurements with solid electrolytes. In: Alcock, C.B. (Ed.), Electromotive Force Measurements in High Temperature Systems. London Inst. Mining and Metallurgy, London, pp. 59–90.

Rickert, H. (Ed.), 1982. Electrochemistry of Solids, An Introduction. Springer-Verlag, New York.

Roseboom, E.H., Kullerud, G., 1958. The solidus in the system Cu–Fe–S between 400 °C and 800 °C. Carnegie Inst. Washington Year Book 57, 222–227.

Sato, M., 1971. Electrochemical measurements and control of oxygen fugacity and other gaseous fugacities with solid electrolyte systems. In: Ulmer, G.C. (Ed.), Research Techniques for High Pressure and High Temperature. Springer-Verlag, New York.

Schneeberg, E.P., 1973. Sulfur fugacity measurements with the electrochemical cell $Ag/AgI/Ag_{2+x}S$, f_{S_2}. Econ. Geol. 68, 507–517.

Scott, S.D., 1973. Experimental calibration of the sphalerite geobarometer. Econ. Geol. 68, 466–474.

Scott, S.D., Barnes, H.L., 1971. Sphalerite geothermometry and geobarometry. Econ. Geol. 66, 653–669.

Sugaki, A., Shima, H., 1965. Synthetic sulfide minerals (II). Mem. Fac. Eng., Yamaguchi Univ. 1, 359–368.

Sugaki, A., Shima, H., Kitakaze, A., Harada, H., 1975. Isothermal phase relations in the system Cu–Fe–S under hydrothermal conditions at 350 °C and 300 °C. Econ. Geol. 70, 806–823.

Thompson, W.T., Flengas, S.M., 1971. Free energies of formation of silver sulfide and lead sulfide by EMF measurements at high temperatures. J. Electrochem. Soc. 118, 419–425.

Toulmin III, P., Barton Jr., P.B., 1964. A thermodynamic study of pyrite and pyrrhotite. Geochim. Cosmochim. Acta. 28, 641–671.

Wagner, C., 1953. Investigations on silver sulfide. J. Chem. Phys. 21, 1819–1827.

West, J.R., 1950. Thermodynamic properties of sulfur. Ind. Eng. Chem. 42, 713–718.

West, W.A., Menzies, A.W.C., 1929. The vapor pressures of sulfur between 100 °C and 550 °C with related thermal data. J. Chem. Phys. 33, 1880–1896.

White, J.L., Orr, R.L., Hultgren, R., 1957. The thermodynamic properties of silver–gold alloys. Acta Metall. 5, 747–760.

Yund, R.A., Kullerud, G., 1966. Thermal stability of assemblages in the Cu–Fe–S system. J. Petrol. 7, 454–488.